Design of viscometers corresponding to a universal molecular simulation method

Kaushik Dayal[1] and Richard D. James[2]†

[1] Civil and Environmental Engineering, Carnegie Mellon University, Pittsburgh, PA 15213, USA

[2] Aerospace Engineering and Mechanics, University of Minnesota, Minneapolis, MN 55455, USA

We present conceptual designs of viscometers corresponding to our new exact molecular simulation method (Dayal & James, *J. Mech. Phys. Solids*, vol. 58 (2), 2010, pp. 145–163). The molecular simulation method is a generalization of the method of Lees & Edwards (*J. Phys.* C: *Solid State Phys.*, vol. 5, 1972, p. 1921), and includes a three-parameter family of incompressible flows, as well as compressible flows and unsteady flows exhibiting vortex stretching. All fluids are allowed. The method gives a way to simulate these flows using relatively few molecules, in the absence of a constitutive relation describing the fluid. This paper presents conceptual designs for viscometers that produce large families of these flows. The basic theme of this paper is that the flows discussed here are a better way to characterize the properties of complex fluids than the currently available methods, such as those based on viscometric flows.

Key words: complex fluids, computational methods, non-continuum effects

---

1. Introduction

In Dumitrica & James (2007) and Dayal & James (2010) we have recently given a method for simulation of fluid flows at the molecular level. It is a significant generalization of the method of Lees & Edwards (1972) for simple shearing flows. Like in Lees & Edwards, only a finite number of atoms are simulated, but all atoms filling all of space satisfy exactly the equations of molecular dynamics. There is no restriction on atomic forces in this method, and it is applicable to classical empirical molecular models up to very general quantum mechanical models, for example, in the most general case, full Born–Oppenheimer quantum mechanics. This method can be used to simulate flows of unusual fluids for which there does not exist a constitutive relation, fluids in regimes currently inaccessible to theory or experiment, fluids undergoing chemical reactions, or fluids for which it is desired to study systematically the influence of the constituents or molecular architecture on properties such as viscosity – in short, the materials science of fluids.

While the method is capable of simulating the dynamics of nanostructures (Dayal & James 2010), the fluid flows that can be simulated by this method have macroscopic Eulerian velocity fields given by the formula

$$v(x, t) = A (I + tA)^{-1} x, \tag{1.1}$$

† Email address for correspondence: james@umn.edu

where A is any 3×3 matrix and t is time, i.e. they are the Eulerian description of so-called affine motions. They can also be considered *homogeneous flows* with a particular time dependence of the coefficient matrix. In this paper we use the terminology *universal flows* because, as explained below, they are exact solutions of the equations of motion of every fluid, subject to zero body force. These flows are generally unsteady, but some special choices of $A \neq 0$ give steady flows.

While multiscale methods like ours would seem to bypass the need for experimental measurement of fluid properties, this is far from true. Experiment has taken on a new urgency with the appearance of this and other multiscale methods. The need for experiment arises from many sources. Most fundamentally, there are significant gaps in the understanding of what level of atomic modelling is needed to simulate a given property in a given fluid accurately, for example, whether pair potentials (with or without a repulsive part), many-body potentials, density functional theory, or full quantum mechanics are required, whether a Langevin approach is adequate, or whether the dynamics of electrons or excited states have to be considered, as is essential in some high-speed flows. Second, there are typically significant length and time scale limitations that remain even after a multiscale method has been designed. It is typically unknown whether, for example, a simulation that delivers a viscosity at a certain shear rate is transferable to lower rates. In our multiscale method there is a trade-off between the number of simulated atoms and the rates that can be achieved under given computational resources.

While our method simulates flows with velocity fields of the form (1.1), we argue that these flows, since they are possible in any fluid (even under extreme conditions as mentioned above), are a fundamental validation tool for all multiscale methods. Since the velocity field is prescribed, then, from an experimental viewpoint, one can design the testing machine without beforehand knowing the properties of the fluid.

The presence of multiscale methods also drives the need for new characterization techniques that directly probe the dynamics of molecules in ways that can validate or refute a dynamic multiscale method. As an example of such a molecular-level prediction, our method implies that the non-equilibrium statistics of molecular motion for these flows, expressed in terms of a molecular density function $f(t, x, v)$, which gives the probability density of finding a molecule at (t, x) with velocity v, satisfies the restriction

$$f(t, x, v) = g(t, v - A(I + tA)^{-1} x) \tag{1.2}$$

for some function $g(t, w)$. Hence, the statistics of the velocity distribution of molecules in the flow (1.1) at one point x_1 at time t uniquely determines its statistics at any other point x_2 at time t. A related consequence of our solutions is that, in the case of a flow-induced chemical reaction, all (macroscopic) points of the fluid reach the initiation point of the reaction at the same time. We use the terminology 'viscometers' for traditional reasons, but it is a comprehensive set of stress measurements and molecular diagnostics that are of interest. An interesting recent example (Chan, Chen & Dunstan 2009) of such an experimental probe that goes beyond stress measurements is the study of molecular shape in Couette flow by the method of fluorescence resonance energy transfer (FRET).

The terminology 'conceptual design' refers to the caveat that we do not give final designs of viscometers. Rather, we describe how best to look at these flows, write their forms in compressible and incompressible cases, consider various interesting phenomena that can be seen in special cases, and discuss what to measure. We identify the surfaces on the boundaries of such flows that undergo simple motions that could be

forced, and, finally, we give some suggestions for the design of viscometers in special cases that we think are most likely to be reducible to practice. We also record the stress and temperature present in such flows, according to some standard continuum theories (Navier–Stokes, viscoelastic, viscous heat-conducting fluid, kinetic theory gas) to give an idea of what stresses are expected on the boundaries in some simple cases. In general, a substantial effort would be required to build and instrument a viscometer that accurately simulates these flows. This effort would be justified by the presence of the universal molecular simulation method and the related fact that the flows produced are exact solutions of the equations of motion for all accepted continuum and mesoscale models of fluids.

As illustrated by Taylor vortices in circular Couette flow, motions of the form (1.1) may not be stable over all rates, i.e. all choices of *A*. The interpretation of this fact for our molecular-level solutions is that the general form of the solution remains the same, but the number of atoms needed to simulate the motion of such a flow beyond the instability becomes very large, too large to be realistically simulated by a molecular-level calculation.

There is a large literature on generalizations of the method of Lees & Edwards (1972). In cases that this literature treats flows other than plane Couette flow, there is no overlap with our method: different flows are treated. Reviews of this literature are given by Todd & Daivis (2007) and Evans & Morriss (2008).

Objective molecular dynamics (OMD) as presented here uses no thermostats. Thus the temperature varies in OMD simulations. An advantage of this is that thermostats are fitted to near-equilibrium behaviour, while OMD can simulate far-from-equilibrium behaviour, such as chemical reactions, combustion and high rates of shear, in which there are substantial temperature changes. A disadvantage of this is that one has to be careful in comparing the results of simulation to experiment where the boundary of the viscometer, say, is being cooled. So, careful consideration of rate, time of simulation and sample size is needed when comparing OMD to experiment. As discussed in Dayal & James (2010), OMD can be used in *some* thermostatted simulations, but the thermostat has to satisfy the invariance conditions needed for atomic forces in OMD.

Many viscometers embody approximations: not all the surfaces in contact with the fluid produce precisely the desired motion. Free surfaces of small area are often present. For the production of universal flows, we could also study approximations. In this first attempt we allow some free surfaces but otherwise try as much as possible to produce the exact motions. Previous experience building testing machines has suggested that rigorous attention to exact predictions is a valuable principle.

2. Objective molecular dynamics

While our molecular simulation method can be developed in the same way for any discrete group of isometries – the main application explored in Dayal & James (2010) was to the stretching of carbon nanotubes at constant strain rate – the main group of interest for fluid mechanics is the *time-dependent translation group*. Thus our presentation will concern only that group. The method is termed *objective molecular dynamics* (OMD) because it relies fundamentally on the frame indifference of the formula for the force on an atom due to all other atoms.

For our purposes the time-dependent translation group is defined as follows. Let e_1, e_2, e_3 be any three linearly independent vectors and let *A* be any linear transformation. Group elements $g_{p,q,r}$ are parametrized by three integers p, q, r. Any such triple corresponds uniquely to a group element. The group elements also depend

on t, $\boldsymbol{e}_1$, $\boldsymbol{e}_2$, $\boldsymbol{e}_3$ and $\boldsymbol{A}$, but this dependence is suppressed. The 'multiplication' rule is

$$g_{p,q,r}\, g_{u,v,w} = g_{p+u,q+v,r+w} \tag{2.1}$$

for any triples of integers p, q, r and u, v, w. Group elements can also act on points $\boldsymbol{x}$ in three-dimensional space at time t: the rule for this action is

$$g_{p,q,r}(\boldsymbol{x}, t) = \boldsymbol{x} + (\boldsymbol{I} + t\boldsymbol{A})(p\boldsymbol{e}_1 + q\boldsymbol{e}_2 + r\boldsymbol{e}_3). \tag{2.2}$$

Geometrically, this represents a time-dependent translation, the time dependence being affine. To simplify the notation below, we write g_ν for g_{ν^1, ν^2, ν^3}, where $\nu = (\nu^1, \nu^2, \nu^3)$ are integers. The element $g_0 = g_{0,0,0}$ is the identity element.

OMD is a consequence of a fundamental (time-dependent) invariant manifold of the equations of molecular dynamics, but it is more easily explained as a computational algorithm. Consider a collection of M atoms termed the *simulated atoms* with time-dependent positions $\boldsymbol{x}_1(t), \ldots, \boldsymbol{x}_M(t)$, $t > 0$. The (infinitely many) remaining atoms are labelled by a double index ν, k, where $\nu \in \mathbb{Z}^3$ and $k \in \{1, \ldots, M\}$. The position of atom ν, k is given at each $t > 0$ in terms of the simulated atoms by applying the group to the simulated atoms using the action (2.2), i.e.

$$\boldsymbol{x}_{\nu,k}(t) = g_\nu(\boldsymbol{x}_k(t), t) = \boldsymbol{x}_k(t) + (\boldsymbol{I} + t\boldsymbol{A})(\nu^1\boldsymbol{e}_1 + \nu^2\boldsymbol{e}_2 + \nu^3\boldsymbol{e}_3). \tag{2.3}$$

Thus the simulated atoms are extended using the instantaneous periodicity defined by the three vectors $((\boldsymbol{I} + t\boldsymbol{A})\boldsymbol{e}_1, (\boldsymbol{I} + t\boldsymbol{A})\boldsymbol{e}_2, (\boldsymbol{I} + t\boldsymbol{A})\boldsymbol{e}_3)$. In the double-index notation the positions of the simulated atoms are given by $\boldsymbol{x}_{0,k}(t) = \boldsymbol{x}_k(t)$.

The basic theorem of OMD says that, if the simulated atoms satisfy the equations of molecular dynamics (with forces given by all the atoms), then, even though the positions of the non-simulated atoms are given by the explicit formula (2.3), they also satisfy exactly the equations of molecular dynamics. To explain this result, we first note that the molecular forces are general but they must satisfy the basic invariances of quantum mechanics. We denote the force on atom ν, k suggestively by the notation $-\partial\varphi/\partial\boldsymbol{x}_{\nu,k}$. In the general case, the formula for atomic forces is required to satisfy the condition of frame indifference, i.e. for all orthogonal $\boldsymbol{Q}$ and $\boldsymbol{c} \in \mathbb{R}^3$,

$$\boldsymbol{Q}\frac{\partial\varphi}{\partial\boldsymbol{x}_{\nu,k}}(\ldots, \boldsymbol{x}_{\nu_1,1}, \ldots, \boldsymbol{x}_{\nu_1,M}, \ldots, \boldsymbol{x}_{\nu_2,1}, \ldots, \boldsymbol{x}_{\nu_2,M}, \ldots)$$

$$= \frac{\partial\varphi}{\partial\boldsymbol{x}_{\nu,k}}(\ldots, \boldsymbol{Q}\boldsymbol{x}_{\nu_1,1} + \boldsymbol{c}, \ldots, \boldsymbol{Q}\boldsymbol{x}_{\nu_1,M} + \boldsymbol{c}, \ldots, \boldsymbol{Q}\boldsymbol{x}_{\nu_2,1} + \boldsymbol{c}, \ldots, \boldsymbol{Q}\boldsymbol{x}_{\nu_2,M} + \boldsymbol{c}, \ldots), \tag{2.4}$$

and also the condition of permutation invariance,

$$\frac{\partial\varphi}{\partial\boldsymbol{x}_{\Pi(\nu,k)}}(\ldots, \boldsymbol{x}_{\nu_1,1}, \ldots, \boldsymbol{x}_{\nu_1,M}, \ldots, \boldsymbol{x}_{\nu_2,1}, \ldots, \boldsymbol{x}_{\nu_2,M}, \ldots)$$

$$= \frac{\partial\varphi}{\partial\boldsymbol{x}_{\nu,k}}(\ldots, \boldsymbol{x}_{\Pi(\nu_1,1)}, \ldots, \boldsymbol{x}_{\Pi(\nu_1,M)}, \ldots, \boldsymbol{x}_{\Pi(\nu_2,1)}, \ldots, \boldsymbol{x}_{\Pi(\nu_2,M)}, \ldots), \tag{2.5}$$

where Π is any permutation that preserves species. Here, preservation of species means that, if $(\mu, k) = \Pi(\nu, \ell)$, then the species (i.e. atomic mass and number) of atom μ, k is the same as the species of atom ν, ℓ. Note that, unlike most treatments of continuum mechanics, quantum mechanics exhibits frame indifference under the full orthogonal group. The conditions of frame indifference and permutation invariance are satisfied for all atomic positions, not just those given by an OMD simulation: hence in (2.4) and (2.5) the subscripts are simply labels of atoms. These invariances are formally satisfied by every accepted model of atomic forces in the

non-relativistic case. As a very general example, they are formally satisfied by the Hellmann–Feynman force formula based on full quantum mechanics under the Born–Oppenheimer assumption. Finally, it is assumed that the mass m_k of simulated atom k is the same as the mass of atom ν, k for any triple of integers ν.

The basic theorem of OMD states that, if $\boldsymbol{x}_1(t), \ldots, \boldsymbol{x}_M(t)$ satisfy the equations of molecular dynamics with any initial conditions, i.e.

$$m_k \ddot{\boldsymbol{x}}_k(t) = -\frac{\partial \varphi}{\partial \boldsymbol{x}_{0,k}}(\ldots, \boldsymbol{x}_{\nu_1,1}(t), \ldots, \boldsymbol{x}_{\nu_1,M}(t), \boldsymbol{x}_{\nu_2,1}(t), \ldots, \boldsymbol{x}_{\nu_2,M}(t), \ldots)$$
$$= -\frac{\partial \varphi}{\partial \boldsymbol{x}_{0,k}}(\ldots, g_{\nu_1}(\boldsymbol{x}_1(t), t), \ldots, g_{\nu_1}(\boldsymbol{x}_M(t), t), g_{\nu_2}(\boldsymbol{x}_1(t), t),$$
$$\ldots, g_{\nu_2}(\boldsymbol{x}_M(t), t), \ldots), \tag{2.6}$$

$$\boldsymbol{x}_k(0) = \boldsymbol{x}_k^0, \quad \dot{\boldsymbol{x}}_k(0) = \boldsymbol{v}_k^0, \quad k = 1, \ldots, M, \tag{2.7}$$

then it follows that all the atoms satisfy the equations of molecular dynamics,

$$m_k \ddot{\boldsymbol{x}}_{\nu,k}(t) = -\frac{\partial \varphi}{\partial \boldsymbol{x}_{\nu,k}}(\ldots, \boldsymbol{x}_{\nu_1,1}(t), \ldots, \boldsymbol{x}_{\nu_1,M}(t), \boldsymbol{x}_{\nu_2,1}(t), \ldots, \boldsymbol{x}_{\nu_2,M}(t), \ldots),$$

$$t > 0, \quad k = 1, \ldots, M, \quad \nu \in \mathbb{Z}^3. \tag{2.8}$$

The initial conditions for the non-simulated atoms are obtained from (2.3) and its time derivative at $t = 0$. The proof of these facts is given in Dayal & James (2010). Both the frame indifference and permutation invariance are used in an essential way. Note that from (2.7), the equations for the simulated atoms comprise a (non-autonomous) finite system of ordinary differential equations in standard form. There are no restrictions on the number of simulated atoms or their the initial conditions. The only restriction on t, $\boldsymbol{A}$, $\boldsymbol{e}_1$, $\boldsymbol{e}_2$, $\boldsymbol{e}_3$ is the condition that $(\boldsymbol{I} + t\boldsymbol{A})\boldsymbol{e}_i$ remain linearly independent; this restriction is discussed in more detail below. At the present time, without introducing approximations of spurious forces, we know of no more general time dependence that can be introduced into the group elements than that given in (2.2).

The multiscale method implied by this theorem is to solve for the simulated atoms only, and keep explicit track of other atoms only insofar as they are needed to calculate the forces on the simulated atoms. Any time that the motion of another atom ν, k is needed, it can be obtained from (2.3). It is expected that a more representative simulation will be obtained with a larger number of simulated atoms. The terminology 'universal' indicates that the number of simulated atoms can be arbitrarily large, and their initial conditions and the atomic forces essentially arbitrary, all associated with a given macroscopic velocity field.

The only conditions on the atomic forces are those that justify the basic existence theorems for equation (2.7) – for example, with typical models for atomic forces, two atoms cannot occupy the same initial position, so initial conditions would have to respect this condition. The possibility of coincidence of atoms is prevented by the repulsive singularity that is built in to typical semi-empirical models of atomic forces. For quantum mechanical descriptions under the Born–Oppenheimer approximation, the nucleus is modelled as a point charge/mass and coincidence of two nuclei is prevented by strong repulsive interactions of the nucleus plus inner electrons. This repulsion does not prevent interaction of valence electrons, which is responsible for bonding and chemical reactions.

The ideas of Kraynik & Reinelt (1992) are useful also in the context of OMD. Although there is no simulation cell in OMD, the simulated atoms can get rather

interspersed with non-simulated atoms, which means that one has to keep track of a large number of non-simulated atoms (i.e. the neighbours). The number can be reduced by using lattice-invariant deformations of the theory of Bravais lattices, as done by Kraynik & Reinelt in simulations of multiphase fluids.

3. Macroscopic motion and statistics of objective molecular dynamics solutions

Despite the fact that the motions of the simulated atoms will vary widely depending on initial conditions and atomic forces, there is certain deterministic information that can be deduced concerning OMD solutions. This deterministic information is independent of the number of simulated atoms and their initial conditions.

We first show that, under a mild additional condition on atomic forces, the centre of mass of the simulated atoms moves with constant velocity. As preparation, we first note that the force on a particular simulated atom $\boldsymbol{x}_k$ is the same as the force on each of its images $\boldsymbol{x}_{\nu,k}$. To prove this, choose a fixed triple of integers $\mu = (\mu^1, \mu^2, \mu^3)$, evaluate the conditions of frame indifference and permutation invariance at the atomic positions (2.3), use permutation invariance (2.5) with $\Pi(\nu, k) = (\nu + \mu, k)$, then use frame indifference (2.4) with $\boldsymbol{Q} = \boldsymbol{I}$ and $\boldsymbol{c} = -\mu^i \boldsymbol{f}_i$, where $\boldsymbol{f}_i = (\boldsymbol{I} + t\boldsymbol{A})\boldsymbol{e}_i$:

$$
\begin{aligned}
&\frac{\partial \varphi}{\partial \boldsymbol{x}_{\nu+\mu,k}}(\ldots, \boldsymbol{x}_{\nu_1,1}, \ldots, \boldsymbol{x}_{\nu_1,M}, \ldots, \boldsymbol{x}_{\nu_2,1}, \ldots, \boldsymbol{x}_{\nu_2,M}, \ldots) \\
&= \frac{\partial \varphi}{\partial \boldsymbol{x}_{\nu,k}}(\ldots, \boldsymbol{x}_{\nu_1+\mu,1}, \ldots, \boldsymbol{x}_{\nu_1+\mu,M}, \ldots, \boldsymbol{x}_{\nu_2+\mu,1}, \ldots, \boldsymbol{x}_{\nu_2+\mu,M}, \ldots) \\
&= \frac{\partial \varphi}{\partial \boldsymbol{x}_{\nu,k}}(\ldots, \boldsymbol{x}_{\nu_1+\mu,1} - \mu^i \boldsymbol{f}_i, \ldots, \boldsymbol{x}_{\nu_1+\mu,M} - \mu^i \boldsymbol{f}_i, \ldots, \boldsymbol{x}_{\nu_2+\mu,1} - \mu^i \boldsymbol{f}_i, \\
&\qquad \ldots, \boldsymbol{x}_{\nu_2+\mu,M} - \mu^i \boldsymbol{f}_i, \ldots) \\
&= \frac{\partial \varphi}{\partial \boldsymbol{x}_{\nu,k}}(\ldots, \boldsymbol{x}_{\nu_1,1}, \ldots, \boldsymbol{x}_{\nu_1,M}, \ldots, \boldsymbol{x}_{\nu_2,1}, \ldots, \boldsymbol{x}_{\nu_2,M}, \ldots).
\end{aligned}
\tag{3.1}
$$

Now we add an additional mild hypothesis on the atomic forces that rules out what at continuum level are considered body forces. We assume that, in any atomic configuration consistent with the ansatz (2.3) of OMD, the force on a region divided by the volume tends to zero as the region gets larger and larger, i.e.

$$
\frac{1}{P^3} \left| \sum_{\nu^1=1}^{P} \sum_{\nu^2=1}^{P} \sum_{\nu^3=1}^{P} \sum_{k=1}^{M} \frac{\partial \varphi}{\partial \boldsymbol{x}_{(\nu^1,\nu^2,\nu^3),k}}(\ldots, \boldsymbol{x}_{\mu_1,1}, \ldots, \boldsymbol{x}_{\mu_1,M}, \ldots, \boldsymbol{x}_{\mu_2,1}, \ldots, \boldsymbol{x}_{\mu_2,M}, \ldots) \right| \\
\to 0
\tag{3.2}
$$

as $P \to \infty$. Now we note that by (3.1) the innermost sum over k in (3.2) is independent of $\nu = (\nu^1, \nu^2, \nu^3)$. Thus the outer sums over ν cancel exactly $1/P^3$, and so (3.2) implies that

$$
\sum_{k=1}^{M} \frac{\partial \varphi}{\partial \boldsymbol{x}_{0,k}}(\ldots, \boldsymbol{x}_{\mu_1,1}, \ldots, \boldsymbol{x}_{\mu_1,M}, \ldots, \boldsymbol{x}_{\mu_2,1}, \ldots, \boldsymbol{x}_{\mu_2,M}, \ldots) = 0,
\tag{3.3}
$$

i.e. the total force on the simulated atoms is zero. Summing the equations of motion for simulated atoms and using the definition of the centre of mass $x_{cm}(t)$, we have that

$$M\ddot{x}_{cm} = \sum_{k=1}^{M} m_k \ddot{x}_k = -\sum_{k=1}^{M} \frac{\partial \varphi}{\partial x_{0,k}} = 0, \tag{3.4}$$

where $M = \sum_k m_k$. All classical models of atomic forces (pair potentials with typically assumed decay at infinity, Tersoff potentials, embedded atom potentials, Stillinger–Weber potentials, any atomic forces with a cut-off) satisfy the condition (3.2). It is expected that (3.2) is also satisfied in a very general quantum mechanical case, too. Equation (3.4) implies that the centre of mass of the simulated atoms moves with constant velocity. It can also be easily seen (using again the invariance) that the equations for the simulated atoms are Galilean invariant. By choosing the initial conditions so that $\dot{x}_{cm}(0) = 0$, then the velocity of the centre of mass remains zero for $t > 0$. We assume below that this has been done.

During a typical simulation, the simulated atoms slowly diffuse into the sea of non-simulated atoms, exhibiting typical molecular diffusion. However, their centre of mass remains fixed. The relationship of all other atoms to the simulated atoms is given by (2.3). We can think of (2.3) at $t = 0$ as defining a periodic Lagrangian grid, $v^1 e_1 + v^2 e_2 + v^3 e_3$, with v^1, v^2, v^3 integers, having typical period of the order of tens of intermolecular dimensions. According to (2.3), this grid is deformed by $x(z, t) = (I + tA)z$, $z = v^i e_i$. Even though all atoms undergo diffusion relative to this deformed grid, the centres of mass of all images of the simulated atoms follow exactly this Lagrangian motion. It is therefore evident that the macroscopic motion in the Lagrangian description of this flow is $x(z, t) = (I + tA)z$ and therefore the velocity in the Eulerian description is

$$v(x, t) = \dot{x}(z^{-1}(x, t), t) = A(I + tA)^{-1} x. \tag{3.5}$$

This velocity field includes some but not all viscometric flows, and it includes many flows that are not viscometric flows.

However, what is of interest here is the connection between these macroscopic motions and atomic-level processes. To examine this in more detail, we note that the equations of motion of the simulated atoms represent a $3M$-dimensional system of highly nonlinear ordinary differential equations. With typical numbers of simulated atoms from 10 to 1000, these are expected to have highly erratic solutions $x_k(t)$, $k = 1, \ldots, M$, that would be modelled statistically at mesoscopic level. However, certain relationships between simulated and non-simulated atoms are deterministic.

To examine this in more detail, we first make an observation about simulated atoms. Initially, these can have any positions and velocities. However, one can redefine the initial positions of the simulated atoms to lie in the unit cell $\mathcal{U} = \{\lambda^i e_i : 0 \leqslant \lambda_i < 1\}$. That is because each simulated atom has an image in this cell, by periodicity, and the image can be taken as the simulated atom. As time proceeds, $\mathcal{U}$ is deformed into $\mathcal{U}_t = (I + tA)\mathcal{U}$. At some time $t^\star$ it may (and typically does) happen that a simulated atom passes out of $\mathcal{U}_{t^\star}$. At that instant, by periodicity, an image of that atom enters the cell from a neighbouring cell. (The velocity of the entering atom $x_{v,k}$ is different from that of the departing atom x_k because of the time dependence on the right-hand side of (2.3).) Now the entering atom can be redefined as a simulated atom. As long as the velocity of the entering atom is taken from (2.3) at $t^\star$, and the simulation restarted at $t^\star$ with the new set of simulated atoms, the full set of atomic motions will be exactly the

same as if this redefinition had not been done. In this way, the simulated atoms can always be assumed to be in the deformed cell $\mathscr{U}_t$.

With this method of handling simulated atoms, it follows from (2.3) that, while the velocities of the simulated atoms $\dot{x}_k(t)$, $k = 1, \ldots, M$, are erratic, the velocities of atoms in the cell $\mathscr{U}_t + (I + tA)v^i e_i$ are determined by those in the cell $\mathscr{U}_t$ according to the following rule: there is an atom in the cell $\mathscr{U}_t + (I + tA)v^i e_i$ with velocity $v + Av^i e_i$ if and only if there is an atom in the cell $\mathscr{U}_t$ with velocity v. This statement is independent of the number of simulated atoms, their initial conditions or the atomic forces. If we pass to mesoscopic level as above by thinking of $z = v^i e_i$ as a Lagrangian position, then this statement becomes: there is an atom near $(I + tA)z$ with velocity $v + Az$ if and only if there is an atom near 0 with velocity v. This has implications for various mesoscale descriptions, but, for example, in the language of the kinetic theory of gases, it says that for these flows the probability of finding an atom at $x = (I + tA)z$ with velocity $v + Az = v + A(I + tA)^{-1}x$ is the same as the probability of finding an atom at 0 with velocity v. In terms of the molecular density function $f(t, x, v)$, this statement is: $f(t, x, v + A(I + tA)^{-1}x) = f(t, 0, v)$. Rearranged, this gives the ansatz (1.2). As noted in Dayal & James (2010) and discussed in more detail below, this ansatz gives an exact reduction of the Boltzmann equation. That is, even though the Boltzmann equation does not inherit everything about molecular dynamics – notably, molecular dynamics is time reversible but the Boltzmann equation is not, see (5.37) – it does inherit precisely the invariant manifold that is the basis of the simulation method described here.

We finish this section with a remark about the singularities of universal flows. The conditions $\det A = 0$, $(\operatorname{tr} A)^2 > 2 \operatorname{tr}(A^2)$ are necessary and sufficient for the avoidance of singularities at all t, i.e. for the condition $\det(I + At) \neq 0$. To see this, write

$$\det(I + tA) = \det(tI) \det\left(\frac{1}{t}I + A\right)$$

$$= (\det A)t^3 + \frac{1}{2}((\operatorname{tr} A)^2 - \operatorname{tr} A^2)t^2 + (\operatorname{tr} A)t + 1. \tag{3.6}$$

The conditions above are necessary and sufficient that this cubic polynomial has no roots for all t.

4. Conceptual design of viscometers

4.1. *Relation to other experimental methods used to study fundamental properties of fluids*

We briefly survey some important methods for determination of properties of fluids and their relation to (1.1). The most commonly used flows used to study fundamental properties of complex fluids are viscometric flows. A subset of these, called *controllable viscometric flows*, are exact solutions of the equations of motion for so-called *simple fluids*, but not, as is the case of (1.1), for all fluids. From a general perspective (Coleman, Markovitz & Noll 1966; Pipkin & Tanner 1972) viscometric flows are flows in which the relative deformation gradient $F_t(x, \tau)$ is expressible in the form

$$F_t(x, \tau) = Q_t(x, \tau)(I + (\tau - t)M_t(x)), \quad M_t^2 = 0, \quad Q_t^{\mathrm{T}} Q_t = I, \quad \tau \leqslant t, \ t > 0. \tag{4.1}$$

The relative deformation gradient is like the ordinary deformation gradient but based on the present configuration as reference: mathematically, it is the gradient with respect to x of $y(y^{-1}(x, t), \tau)$ where $y(z, t)$ is the ordinary Lagrangian description

of motion. Viscometric flows have the geometric interpretation as motions that locally look like simple shearing flows, but the shearing direction and the normal to the slip surfaces can change from point to point. The controllable viscometric flows (Yin & Pipkin 1970) consist of simple shearing flow, shearing between tilted planes, and a certain flow in a sector between concentric cylinders. If macroscopic inertia is neglected, there are two additional controllable flows: helicoidal flows and a certain flow with slip surfaces that curl up (Yin & Pipkin 1970). One example of helicoidal flows is torsional flow, used in the parallel-plate viscometer. Many viscometers, such as the widely used cone-and-plate viscometer, produce controllable flows with inertia neglected, but have velocity fields that are not known beforehand. However, typically, the slip surfaces are known, and this, together with suitable measurement of the velocities of these known slip surfaces, is sufficient to measure one or more of the viscometric functions that characterize the stress response (Pipkin & Tanner 1972).

We now determine if there are any viscometric flows that are universal flows. In the definition (4.1), the condition $\boldsymbol{M}_t^2 = 0$ implies that $\boldsymbol{M}_t$ is expressible in the form $\boldsymbol{M}_t = \boldsymbol{a}_t \otimes \boldsymbol{b}_t \neq 0$, with $\boldsymbol{a}_t \cdot \boldsymbol{b}_t = 0$. It then follows from (4.1) that such flows are incompressible, $\det \boldsymbol{F}_t = 1$. On the other hand, the relative deformation gradient of a universal flow (1.1) is

$$\boldsymbol{F}_t(\boldsymbol{x}, \tau) = (\boldsymbol{I} + \tau \boldsymbol{A})(\boldsymbol{I} + t\boldsymbol{A})^{-1} \quad (4.2)$$

by direct calculation. Now compare $\boldsymbol{F}_t^{\mathrm{T}} \boldsymbol{F}_t$ from (4.2) with that from the definition of viscometric flows, evaluated at $t = 0$:

$$(\boldsymbol{I} + \tau \boldsymbol{M}_0)^{\mathrm{T}}(\boldsymbol{I} + \tau \boldsymbol{M}_0) = (\boldsymbol{I} + \tau \boldsymbol{A})^{\mathrm{T}}(\boldsymbol{I} + \tau \boldsymbol{A}), \quad \tau < t. \quad (4.3)$$

Differentiating this once at $\tau = 0$ and then twice with respect to τ gives the pair of necessary and sufficient conditions,

$$\boldsymbol{A} + \boldsymbol{A}^{\mathrm{T}} = \boldsymbol{a}_0 \otimes \boldsymbol{b}_0, \quad \boldsymbol{A}^{\mathrm{T}} \boldsymbol{A} = |\boldsymbol{a}_0|^2 \, \boldsymbol{b}_0 \otimes \boldsymbol{b}_0. \quad (4.4)$$

The first of these implies the existence of a skew tensor $\boldsymbol{W}$ satisfying $\boldsymbol{A} = \boldsymbol{W} + \boldsymbol{a}_0 \otimes \boldsymbol{b}_0$. Then the second of (4.4) becomes

$$\boldsymbol{W}^2 = -\boldsymbol{W} \boldsymbol{a}_0 \otimes \boldsymbol{b}_0 - \boldsymbol{b}_0 \otimes \boldsymbol{W} \boldsymbol{a}_0. \quad (4.5)$$

Operate (4.5) on $\boldsymbol{a}_0$ and use $\boldsymbol{b}_0 \cdot \boldsymbol{a}_0 = \boldsymbol{a}_0 \cdot \boldsymbol{W} \boldsymbol{a}_0 = 0$ to get $\boldsymbol{W}^2 \boldsymbol{a}_0 = 0$. A non-zero skew tensor has a unique axis, so we must therefore have $\boldsymbol{W} \boldsymbol{a}_0 = 0$. Together with (4.5) this implies that $\boldsymbol{W} = 0$, and we finally get that $\boldsymbol{A} = \boldsymbol{a}_0 \otimes \boldsymbol{b}_0$, $\boldsymbol{a}_0 \cdot \boldsymbol{b}_0 = 0$.

However, we can now see that the intersection between viscometric flows and universal flows is only simple shearing flows. That is, $\boldsymbol{A} = \boldsymbol{a}_0 \otimes \boldsymbol{b}_0$ implies that $(\boldsymbol{I} + t\boldsymbol{a}_0 \otimes \boldsymbol{b}_0)^{-1} = \boldsymbol{I} - t\boldsymbol{a}_0 \otimes \boldsymbol{b}_0$, and, since $\boldsymbol{a}_0 \cdot \boldsymbol{b}_0 = 0$, these flows are therefore

$$\boldsymbol{v}(\boldsymbol{x}, t) = \boldsymbol{A}(\boldsymbol{I} + t\boldsymbol{A})^{-1} \boldsymbol{x} = (\boldsymbol{b}_0 \cdot \boldsymbol{x})\boldsymbol{a}_0, \quad \boldsymbol{a}_0 \cdot \boldsymbol{b}_0 = 0. \quad (4.6)$$

It also can be shown (Dayal & James 2010) that the intersection of universal flows with so-called motions with constant principal relative stretch histories is also (4.6). In summary, though viscometric flows have been the workhorse of experimental fluid mechanics of complex fluids, it can be argued that universal flows are better for various reasons: (*a*) there is an exact molecular-level simulation method; (*b*) unlike viscometric flows, they are exact solutions for all continuum and mesoscale models of fluids (see § 5); and (*c*) there are more free parameters than viscometric flows that can be used to test continuum, mesoscale or atomistic models.

An interesting apparatus invented by Taylor (1934) is the four-roll mill. It has been used to study drop deformation and breakup (Taylor 1934), rheology of viscoelastic

liquids (Parlato 1969), flow-induced changes in the conformation of macromolecules (Crowley *et al.* 1976) and shear-induced crystallization (Torza 1975), and has been developed extensively by Leal and collaborators (Bentley & Leal 1986). This device produces – ideally, but see Giesekus (1962) and Lagnado & Leal (1990) – two-dimensional flows of the form $v(x, t) = Gx$, where

$$G = \frac{E}{2} \begin{pmatrix} 1 + \lambda & 1 - \lambda & 0 \\ -(1 - \lambda) & -(1 + \lambda) & 0 \\ 0 & 0 & 0 \end{pmatrix} \qquad (4.7)$$

in a rectangular Cartesian coordinate system. To find the intersection of these flows with universal flows, we first note that they are all steady. This intersection is characterized by the equation $A(I + tA)^{-1} = G$, i.e. $A = G(I + tA)$. This in turn is equivalent to $G = A$, $A^2 = 0$. As noted above in a different context, this is equivalent to $A = a \otimes b$, $a \cdot b = 0$, and therefore these lead back to simple shearing flows. (This argument also shows that the only steady universal flows are simple shearing flows.) The simple shearing flows are included in (4.7) as the case $\lambda = 0$.

In summary, except for simple shearing flows, universal flows seem to be unexplored in devices to measure fundamental properties of fluids.

4.2. *Universal flows confined by rigid surfaces*

The design of devices to study fundamental properties of fluids is greatly aided by having (possibly curved) surfaces that move as rigid bodies on which the no-slip condition can be imposed. We analyse this possibility here. Obviously, simple shearing flow is an example.

At each time $t > 0$, such a surface must consist of the same material particles of the fluid, and therefore will have to be independent of time in the Lagrangian description. In the notation of this paper, it will therefore be describable in the form

$$z(u_1, u_2), \quad u_1, u_2 \in \mathcal{D}, \qquad (4.8)$$

where $\mathcal{D}$ is a domain in two dimensions and the derivatives $z_{,1}$ and $z_{,2}$ are linearly independent. Let the universal flow be given by $x(z, t) = (I + tA)z$ for some 3×3 matrix A. The surface described by (4.8) undergoes a rigid motion if and only if there is the time-dependent rotation matrix $R(t)$ and translation $c(t)$ such that

$$(I + tA)z(u_1, u_2) = R(t)z(u_1, u_2) + c(t). \qquad (4.9)$$

Evaluating this at, say, $z_0 = z(0, 0)$ we get a formula for $c(t)$:

$$c(t) = (I + tA)z_0 - R(t)z_0. \qquad (4.10)$$

Replacing this back into (4.9) and differentiating with respect to u_1, u_2, we have

$$(I + tA)z_{,1} = R(t)z_{,1}, \qquad (4.11a)$$
$$(I + tA)z_{,2} = R(t)z_{,2}. \qquad (4.11b)$$

Dot these equations by themselves and get

$$|R(t)z_{,1}|^2 = |z_{,1}|^2 = |(I + tA)z_{,1}|^2 = |z_{,1}|^2 + 2tz_{,1} \cdot Az_{,1} + t^2 |Az_{,1}|^2, \qquad (4.12a)$$
$$|R(t)z_{,2}|^2 = |z_{,2}|^2 = |(I + tA)z_{,2}|^2 = |z_{,1}|^2 + 2tz_{,2} \cdot Az_{,2} + t^2 |Az_{,2}|^2. \qquad (4.12b)$$

The left-hand sides are independent of t. Clearly, then, the right-hand sides are independent of t if and only if $Az_{,1} = Az_{,2} = 0$. Since $z_{,1}$ and $z_{,2}$ are linearly independent, this is equivalent to the statement that A is a matrix of rank one, that is,

it is expressible in the form $\boldsymbol{A} = \boldsymbol{a} \otimes \boldsymbol{n}$. The null space of $\boldsymbol{A}$ is a plane (perpendicular to $\boldsymbol{n}$) and $\boldsymbol{z}_{,1}$ and $\boldsymbol{z}_{,2}$ lie on this plane for all choices of $u_1, u_2 \in \mathscr{D}$. This shows that the surface $\boldsymbol{z}(u_1, u_2)$ itself must be a plane with normal $\boldsymbol{n}$, $|\boldsymbol{n}| = 1$. Without loss of generality we can reparametrize this plane and write

$$\boldsymbol{z}(u_1, u_2) = u_1 \boldsymbol{e}_1 + u_2 \boldsymbol{e}_2 + \boldsymbol{z}_0, \quad \boldsymbol{e}_1 \cdot \boldsymbol{n} = \boldsymbol{e}_2 \cdot \boldsymbol{n} = 0, \tag{4.13}$$

with $\boldsymbol{e}_1, \boldsymbol{e}_2$ orthonormal. Now (4.11) becomes

$$\boldsymbol{e}_1 = \boldsymbol{R}(t)\boldsymbol{e}_1, \tag{4.14a}$$
$$\boldsymbol{e}_2 = \boldsymbol{R}(t)\boldsymbol{e}_2, \tag{4.14b}$$

implying that $\boldsymbol{R} = \boldsymbol{I}$: the plane just translates. The only remaining freedom of the choice of the plane is the choice of the constant vector $\boldsymbol{z}_0$. Thus there are a family of parallel planes with normal $\boldsymbol{n}$ that are translated by the flow. The motion of these planes is given by the formula

$$\boldsymbol{x}(u_1, u_2, t) = (\boldsymbol{I} + t\boldsymbol{A})\boldsymbol{z}(u_1, u_2) = u_1 \boldsymbol{e}_1 + u_2 \boldsymbol{e}_2 + \boldsymbol{z}_0 + t(\boldsymbol{z}_0 \cdot \boldsymbol{n})\boldsymbol{a}. \tag{4.15}$$

The planes are translated in the direction $\boldsymbol{a}$ at constant speed $|\boldsymbol{a}| \boldsymbol{z}_0 \cdot \boldsymbol{n}$.

There are two subcases.

4.2.1. *Simple shearing* ($\boldsymbol{a} \cdot \boldsymbol{n} = 0$)

If $\boldsymbol{A} = \boldsymbol{a} \otimes \boldsymbol{n}$ with $\boldsymbol{a} \cdot \boldsymbol{n} = 0$ we can write $\boldsymbol{a} = |\boldsymbol{a}| \boldsymbol{e}_1$, $\boldsymbol{n} = |\boldsymbol{n}| \boldsymbol{e}_3$ for orthonormal vectors $\boldsymbol{e}_1, \boldsymbol{e}_3$ (consistent with the description of the plane above) and put $\kappa = |\boldsymbol{a}||\boldsymbol{n}|$, so that $\boldsymbol{A} = \kappa \boldsymbol{e}_1 \otimes \boldsymbol{e}_3$. In the Eulerian description the velocity field is

$$\boldsymbol{v}(\boldsymbol{x}, t) = \boldsymbol{A}(\boldsymbol{I} + t\boldsymbol{A})^{-1}\boldsymbol{x} = (\kappa \boldsymbol{e}_1 \otimes \boldsymbol{e}_3)(\boldsymbol{I} - \kappa \boldsymbol{e}_1 \otimes \boldsymbol{e}_3)\boldsymbol{x} = \kappa x_3 \boldsymbol{e}_1. \tag{4.16}$$

This is simple shearing flow, with κ being the shear rate. This needs no further analysis.

4.2.2. *Pressure shear* ($\boldsymbol{a} \cdot \boldsymbol{n} \neq 0$)

If $\boldsymbol{A} = \boldsymbol{a} \otimes \boldsymbol{n}$ with $\boldsymbol{a} \cdot \boldsymbol{n} \neq 0$ we have $(\boldsymbol{I} + t\boldsymbol{A})^{-1} = \boldsymbol{I} - ((\boldsymbol{a} \cdot \boldsymbol{n})t/(1 + (\boldsymbol{a} \cdot \boldsymbol{n})t))\boldsymbol{a} \otimes \boldsymbol{n}$ and so the velocity field is

$$\boldsymbol{v}(\boldsymbol{x}, t) = \frac{1}{1 + (\boldsymbol{a} \cdot \boldsymbol{n})t}(\boldsymbol{n} \cdot \boldsymbol{x})\boldsymbol{a}, \quad t > 0. \tag{4.17}$$

This unsteady, compressible flow has a singularity at $t = -1/\boldsymbol{a} \cdot \boldsymbol{n}$ if $\boldsymbol{a} \cdot \boldsymbol{n} < 0$. Using (4.15), it is seen that this velocity field is consistent with the homogeneous flow between two parallel plates with normal $\boldsymbol{n}$ moving towards ($\boldsymbol{a} \cdot \boldsymbol{n} < 0$) or away from ($\boldsymbol{a} \cdot \boldsymbol{n} > 0$) each other. The fluid velocity is always in the direction $\boldsymbol{a}$ of motion of the plates. The singularity that occurs in the case $\boldsymbol{a} \cdot \boldsymbol{n} < 0$ is associated physically with the plates striking each other. Obviously, a viscometer could only produce a reasonable representation of such a flow up to a time somewhat less than $t = -1/\boldsymbol{a} \cdot \boldsymbol{n} > 0$ when this singularity occurs.

Schematically, a viscometer that produces this flow is shown in figure 1 and can be termed a *pressure-shear viscometer*. The case pictured is with $\boldsymbol{a} \cdot \boldsymbol{n} < 0$. Referring to figure 1, the key feature that such a viscometer must exhibit is that *the leading edge of plate 1 must move at constant velocity*.

Referring to figure 1 we distinguish two regimes.

(*a*) Low-speed regime. For pressures not too far from room pressure and velocities less than tens of metres per second, wave propagation effects are suppressed and one can consider a relatively simple design. A commercially available solution is
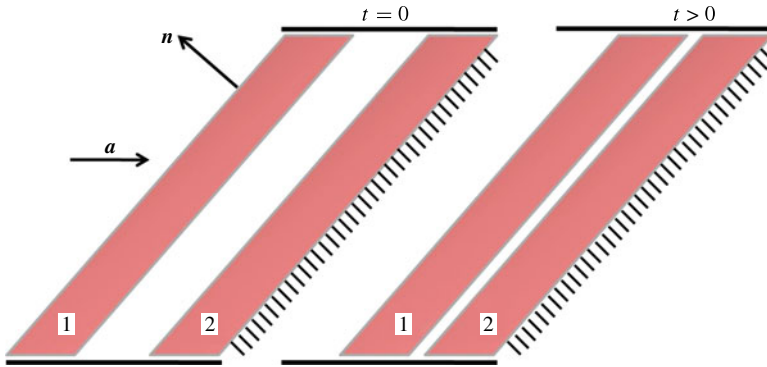
FIGURE 1. (Colour online available at journals.cambridge.org/flm) Schematic pressure-shear viscometer: vectors $\boldsymbol{a}$ and $\boldsymbol{n}$ as in the text. The leading edge of plate 1 moves *at constant velocity* in the direction $\boldsymbol{a}$ towards plate 2, which is stationary. Both plates are in general oblique to the velocity as shown.

a high-rate servohydraulic testing machine. These have feedback control systems that can be used to keep the velocity of plate 1 constant. The duration of the test would then be determined by practical considerations relating to the constancy of this velocity, i.e. machine performance. It is extremely interesting in such experiments to run series of tests that vary independently both the magnitude of the speed $|\boldsymbol{a}||\boldsymbol{n}|$ as well as the obliqueness $\boldsymbol{a} \cdot \boldsymbol{n}$.

(b) High-speed regime. In this regime, wave propagation effects become important and completely different design considerations are needed. The challenges can be divided into two categories: (i) the management of transients and (ii) strategies to maintain the approximate constancy of velocity of the leading edge of plate 1. The solution of (i) has been considered in great detail in the shock physics community, and concerns the assignment of dimensions and velocities so that, early in the test, a sufficient number of wave reflections occur in the material to 'shock it up' to a homogeneously deforming state. As far as we can determine, (ii) has not been considered in the shock physics community, even though the solutions described here are also valid in all solids and the advantages of having a corresponding molecular-level simulation are arguable in that case too. A naive solution in the case of compressible fluids is the following: use high-strength plates, ignore the deformation of the plates themselves, and make them so massive that, for the duration of the test, the reaction force of the fluid on plate 1 causes a negligible slow-down. To briefly examine this possibility, write Newton's laws for the incoming plate with force produced by the compressing fluid in the gap. For the simplest model of a monatomic gas being compressed adiabatically, the dimensionless form of the equation of motion of the incoming plate is

$$\ddot{\xi} = c\xi^{-\gamma}, \quad \xi(0) = 1, \quad \dot{\xi}(0) = -1, \quad c = \frac{(\boldsymbol{a} \cdot \boldsymbol{n})p_0 x_0}{\rho h v_0^2 |\boldsymbol{a}||\boldsymbol{n}|}, \qquad (4.18)$$

where $\gamma = 5/3$, p_0 is the initial pressure, $x_0 < 0$ is the initial position of the leading edge of the plate, v_0 is its initial velocity, ρ is the density of the plate material, h is the thickness of the plate, the dimensionless position is $\xi = x/x_0$ and the dimensionless time is $\tau = -(v_0/x_0)t$. As a particular example, a steel plate of 1 cm thickness at $45°$ with initial velocity 1000 m s^{-1} and initial gap of 1 cm

only slows down by 1.3 m s^{-1} after travelling through 99.9 % of the gap, at which point the pressure is up to about 10 GPa. A more sophisticated analysis takes into account wave propagation in the plates. We have noticed (not presented here) that, by designing an elastically inhomogeneous flyer plate with spatial variation of Young's modulus matched to the properties of the gas, it is possible to maintain approximately constant velocity of the leading edge of plate 1, even while its centre of mass slows down.

Because it is applicable to high-speed flows and compressible fluids, and it has the potential to produce extreme conditions of temperature, chemical reactions, dissociation and excited electronic states, this case is quite interesting. It also provides an interesting experimental method to study, from an atomistic viewpoint, the processes occurring in an internal combustion engine. However, the motion of a cylinder in an internal combustion engine does not occur at constant velocity, so, for accurate simulation, a device of the type discussed is needed.

4.3. *General incompressible universal flows*

For many liquids or highly elastic solids, the constraint of incompressibility is reasonable. The case of simple shearing flow is incompressible. Here, we find all universal flows that are incompressible and consider the possibility of viscometers based on them.

We impose the condition of incompressibility, which in Lagrangian form is $\det(\boldsymbol{I} + t\boldsymbol{A}) = 1$ for all $t > 0$. Divide this by t^3 and consider the characteristic equation. One sees immediately that necessary and sufficient conditions for $\det(\boldsymbol{I} + \boldsymbol{A}t) = 1$ for all $t > 0$ are that $\det \boldsymbol{A} = \operatorname{tr} \boldsymbol{A} = \operatorname{tr} \boldsymbol{A}^2 = 0$. By direct calculation in a suitable orthonormal basis in which the second vector is a null vector of $\boldsymbol{A}$, necessary and sufficient conditions that $\det \boldsymbol{A} = \operatorname{tr} \boldsymbol{A} = \operatorname{tr} \boldsymbol{A}^2 = 0$ are that

$$\boldsymbol{A} = \begin{pmatrix} 0 & 0 & \kappa \\ \gamma_1 & 0 & \gamma_3 \\ 0 & 0 & 0 \end{pmatrix} \tag{4.19}$$

in this basis. Generally, this is a rank-two matrix, so there are many universal flows that are not viscometric flows. In its general (most interesting) rank-two form, universal incompressible flows do not rigidly deform any surfaces, by the results of § 4.2.

In abstract form, (4.19) is $\boldsymbol{A} = \kappa \boldsymbol{e}_1 \otimes \boldsymbol{e}_3 + \boldsymbol{e}_2 \otimes \boldsymbol{g}$, where $\boldsymbol{e}_1, \boldsymbol{e}_2, \boldsymbol{e}_3$ are orthonormal and $\boldsymbol{g} = \gamma_1 \boldsymbol{e}_1 + \gamma_3 \boldsymbol{e}_3$. A short calculation shows that $\boldsymbol{A}(\boldsymbol{I} + t\boldsymbol{A})^{-1} = \boldsymbol{A} - \kappa t \gamma_1 \boldsymbol{e}_2 \otimes \boldsymbol{e}_3$. Therefore the Eulerian description of this motion is

$$\boldsymbol{v}(\boldsymbol{x}, t) = \boldsymbol{A}\boldsymbol{x} - \kappa t \gamma_1 y_3 \boldsymbol{e}_2. \tag{4.20}$$

The velocity gradient is $\boldsymbol{A} - \kappa t \gamma_1 \boldsymbol{e}_2 \otimes \boldsymbol{e}_3$ and the vorticity is

$$\operatorname{curl} \boldsymbol{v} = (\gamma_3 - \kappa \gamma_1 t)\boldsymbol{e}_1 - \kappa \boldsymbol{e}_2 - \gamma_1 \boldsymbol{e}_3. \tag{4.21}$$

Hence, if $\kappa \gamma_1 \neq 0$ the vorticity grows linearly in time, an interesting feature not produced by other viscometers, to our knowledge. This can be attributed to vortex line stretching. The vorticity is, of course, independent of position.

To visualize this motion, it seems simplest to consider a rectangular solid with faces normal to the axes $\boldsymbol{e}_1, \boldsymbol{e}_2, \boldsymbol{e}_3$. It may be desirable to choose particular edge lengths of this solid, but for further simplicity we consider the unit cube. A typical motion of this cube corresponding to choices of $\kappa, \gamma_1, \gamma_3$ is shown in figure 2.
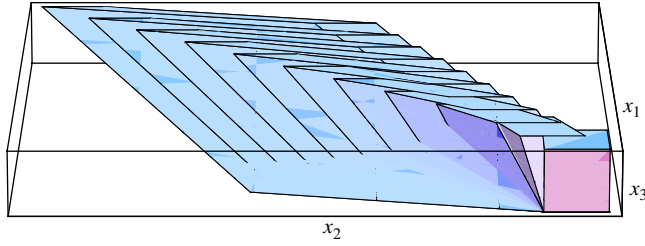
FIGURE 2. (Colour online) Universal flow of the unit cube having outer normals e_1, e_2, e_3. The values of the parameters are $\kappa = 1.4$, $\gamma_1 = 0.9$, $\gamma_3 = 0.7$. The figure shows the same set of material particles at successive instants of time. Time between pictures is 0.5 in consistent units.
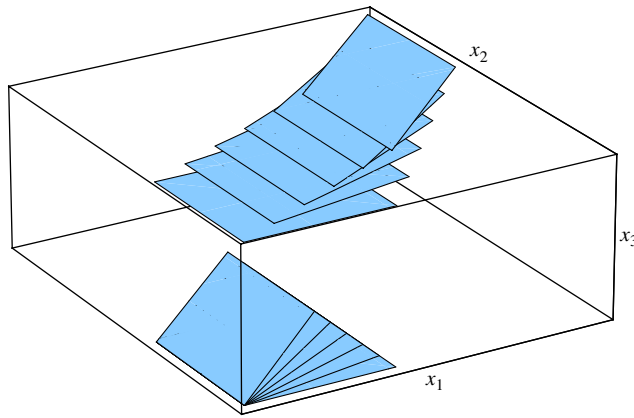

FIGURE 3. (Colour online) Motion of the two planes with normal e_3 with parameters chosen as in figure 2. Time between pictures is 0.2 in consistent units.

Note that $e_3 \cdot (I + tA)z = e_3 \cdot z$. Thus, in the macroscopic description, material particles in planes with normal e_3 remain in those planes. In particular, the two faces of the unit cube with normals $\pm e_3$ remain in their planes. The motion is homogeneous, so that each of these square faces becomes a parallelogram. Again, from the formula $x(z, t) = (I + tA)z$, the face on the particular plane $z \cdot e_3 = 0$ undergoes the motion $(I + te_2 \otimes g)z$, i.e. simple shearing. Otherwise, the in-plane motions generally differ in each plane. Typical motions of the two faces with normal e_3 (corresponding to the same choice of parameters as in figure 2) are shown in figure 3.

Consider points in a plane $x_3 = c = const.$, for example, the four corners of one of the initial squares shown in figure 3. Such points undergo the motion $z \rightarrow z + t(c\kappa e_1 + (g \cdot z)e_3)$. As do all points in a universal flow, such points move with constant velocity in a straight line. But this formula has an additional feature that may facilitate construction of a device: all points on the plane $x_3 = c$ have the same velocity in the e_1 direction. Thus, to produce the motion of the top plate, one could conceive of a rigid body moving in the e_1 direction (to the right in figure 3) with constant velocity, and tracks attached to it with various velocities (each of value $g \cdot z$) in the perpendicular e_2 direction: this idea is developed in the next subsection. A second simplifying feature of the motion of any subset of the plane $x_3 = const.$ is that
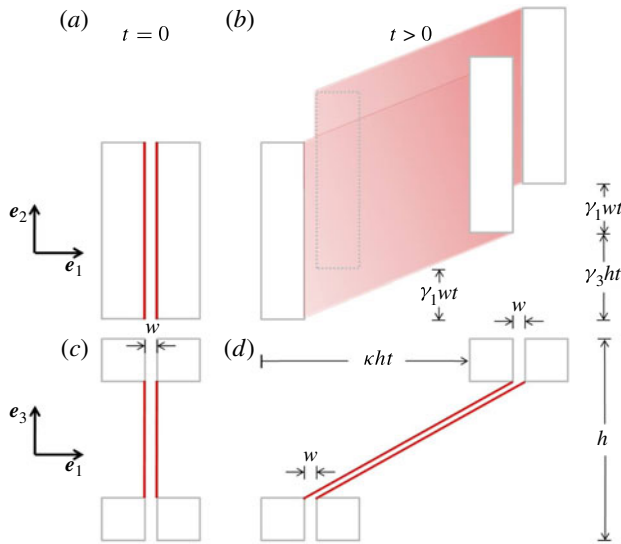
FIGURE 4. (Colour online) Conceptual viscometer for universal flows in the incompressible case: (*a,b*) top views; (*c,d*) side views; (*a,c*) at $t = 0$; (*b,d*) at $t > 0$. Deformable membranes are in dark grey (red). The fluid to be tested is confined to the gap between the dark grey (red) membranes. The parameters w, h are assignable dimensions and κ, γ_1, γ_3 are the elements of the matrix **A** in the representation (4.19).

it is area-preserving. Planes not of the form $x_3 = const.$ can undergo substantial area changes, as seen in figure 2.

4.3.1. *A conceptual viscometer for incompressible universal flows*

Every viscometer has surfaces that do not impose the intended motion on the fluid. In successful designs, these are typically confined to small areas far from the place where measurements are taken. As explained above, general incompressible universal flows are not bounded by any surfaces that undergo rigid motions. Thus, we infer that it is essential that some surfaces bounding the flow are deformable. To achieve the large motions desirable for a viscometer, the obvious choices of such surfaces are highly elastic membranes.

For the same reason that universal flows are possible in every fluid, they are exact solutions for theories of (uniform) membranes, for example, the dynamic membrane theory of nonlinear elasticity. This is also true for membranes loaded by the same uniform stress on each side.

One possible concept is pictured in figure 4. It consists of two membranes, each stretched between two rigid blocks. The blocks are required to move in a precise manner so that the membranes shear, and the distance between membranes also changes, as shown. The labelling of values κ, γ_1, γ_3 corresponds to the entries in the matrix **A** of (4.19) that corresponds to this flow.

To attain large shearing of the fluid under modest stretching of the membrane, the dimension w can be small. If there is substantial stress imposed on the membrane by the fluid, it should be backed up by a stiff plate. A constant velocity can be imposed on the whole structure to keep a portion of the fluid in a fixed viewing region.
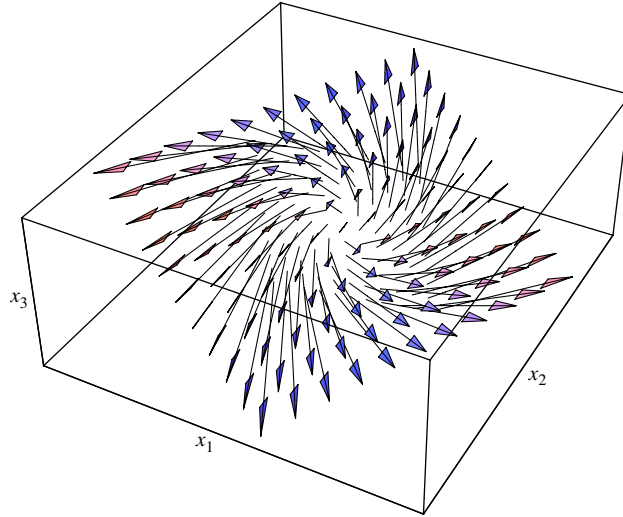
FIGURE 5. (Colour online) Vortex-like structure; $\kappa = -1.3$, $\gamma_1 = 1.3$, $\gamma_3 = 0.7$, $t = 0.1$. The velocity field on the plane $x_2 = const.$ is shown, and this velocity field is independent of x_2. The line perpendicular to this plane passing through the centre of this structure is a line of zero velocity.

4.3.2. *Vortex-like structures*

The vector fields of some incompressible velocity fields given by (4.19) and (4.20), restricted to suitable planes, appear to show a vortex. An example on one such plot viewed from the $(1.3, -2.4, 2)$ direction is seen in figure 5. According to all the standard definitions, this is not a vortex. The various definitions in common usage, together with their evaluation for the present motion with general choices of the parameters, are summarized in table 1. These are easily obtained from the formulae

$$\nabla \boldsymbol{v} = \begin{pmatrix} 0 & 0 & \kappa \\ \gamma_1 & 0 & \gamma_3 - \kappa\gamma_1 t \\ 0 & 0 & 0 \end{pmatrix}, \quad \boldsymbol{D} = \frac{1}{2}(\nabla\boldsymbol{v} + \nabla\boldsymbol{v}^{\mathrm{T}}), \quad \boldsymbol{W} = \frac{1}{2}(\nabla\boldsymbol{v} - \nabla\boldsymbol{v}^{\mathrm{T}}), \quad (4.22)$$

$$\boldsymbol{M} = \frac{\partial \boldsymbol{D}}{\partial t} + (\nabla\boldsymbol{D})\boldsymbol{v} + \boldsymbol{D}\nabla\boldsymbol{v} + (\nabla\boldsymbol{v})^{\mathrm{T}}\boldsymbol{D}, \quad Z = \{\boldsymbol{e} : \boldsymbol{e} \cdot \boldsymbol{D}\boldsymbol{e} = 0\}. \quad (4.23)$$

Hence, it is seen that this is not a vortex, though it is a limiting case of a vortex according to all the definitions (so is simple shearing flow), except the M_Z criterion. All the eigenvalues of $\nabla\boldsymbol{v}$ are zero, so the criteria of Chakraborty, Balachandar & Adrian (2005) are also not satisfied. In summary, in the incompressible case, our method does not give a way to simulate vortex motion, as vortices are usually defined.

In compressible cases of universal flows, there are a great many vortices satisfying all of these definitions. More generally, every example in the general classification of critical points of flows of Chong *et al.* (1990) can be achieved at a given time by a particular choice of $\boldsymbol{A}$. For example, the choice $\boldsymbol{A} = (\boldsymbol{I} - \boldsymbol{D})^{-1}\boldsymbol{D}$, where $\boldsymbol{D} = \mathrm{diag}(\lambda_1, \lambda_2, \lambda_3)$, gives the velocity gradient $\nabla\boldsymbol{v} = \mathrm{diag}(\lambda_1, \lambda_2, \lambda_3)$ at $t = 1$.

Name	Criterion for a vortex	Value	Reference
Q criterion	$Q = (1/2)(|\boldsymbol{W}|^2 - |\boldsymbol{D}|^2) > 0$	$Q = 0$	Hunt, Wray & Moin (1988)
Δ criterion	$\Delta = (Q/3)^3 + (\det \nabla \boldsymbol{v}/2)^2 > 0$	$\Delta = 0$	Chong, Perry & Cantwell (1990)
λ_2 criterion	$\lambda_2(\boldsymbol{D}^2 + \boldsymbol{W}^2) < 0$	$\lambda_2 = 0$	Jeong & Hussain (1995)
M_Z criterion	$\boldsymbol{e} \cdot \boldsymbol{Me}$ indefinite on Z	$\boldsymbol{e} \cdot \boldsymbol{Me} > 0$ on Z	Haller (2005)

TABLE 1. Evaluation of various criteria for the presence of a vortex based on the motion $\boldsymbol{v}(\boldsymbol{x}, t) = \boldsymbol{Ax} - \kappa t \gamma_1 y_3 \boldsymbol{e}_2$, with $\boldsymbol{A}$ given by (4.19), for general choices of parameters $\kappa, \gamma_1, \gamma_3$.

5. Stresses according to some conventional continuum and mesoscopic theories

While the primary purpose of the proposed devices are to give experimental tests of atomic-level simulations, it is useful to calculate the stresses given by these motions for several familiar continuum and mesoscale theories. As explained above, $\boldsymbol{v}(\boldsymbol{x}, t) = \boldsymbol{A}(\boldsymbol{I} + t\boldsymbol{A})^{-1} \boldsymbol{x}$ identically satisfies the equations of motion of all accepted continuum theories of fluid (and solid) mechanics. In most cases below this is easily seen from the calculation

$$\rho(\boldsymbol{v}_t + \nabla \boldsymbol{v} \boldsymbol{v}) = \rho \left(-\boldsymbol{A}(\boldsymbol{I} + \boldsymbol{A}t)^{-1} \boldsymbol{A}(\boldsymbol{I} + \boldsymbol{A}t)^{-1} \boldsymbol{x} + \boldsymbol{A}(\boldsymbol{I} + \boldsymbol{A}t)^{-1} \boldsymbol{A}(\boldsymbol{I} + \boldsymbol{A}t)^{-1} \boldsymbol{x} \right)$$
$$= 0 \tag{5.1}$$

and the observation that the stress only depends on t so that $\mathrm{div}\,\sigma = 0$. In the case of incompressible fluids, the pressure can be taken as constant. It can be stated that all accepted theories of fluid behaviour faithfully inherit the invariant manifold of molecular dynamics described in §2. For thermodynamic theories, again motivated by the results in §2, add the condition that the temperature only depends on time, $\theta = \theta(t)$. Unlike the velocity field, the temperature $\theta(t)$ is material-dependent, or, in the atomic-level setting of §2, dependent on the expression for the atomic forces. In continuum theories it is determined by the energy equation, which reduces to an ordinary differential equation parametrized by $\boldsymbol{A}$. In OMD calculations, if the mean kinetic energy of the atoms (after subtraction of the mean velocity) is taken to represent the temperature, then the temperature is obtained by a simple sum $\sum_{k=1}^{M}(1/2)m_k |\dot{\boldsymbol{x}}_k|^2$ over the simulated atoms, assumed that the normalization $\dot{\boldsymbol{x}}_{cm}(0) = 0$ described after (3.4) has been done (see the remark about units following equation (8.3) of Dayal & James 2010). For mixture theories, one adds that the diffusive fluxes vanish.

5.1. *Incompressible fluids*

In this case we express all components in the basis $\boldsymbol{e}_1, \boldsymbol{e}_2, \boldsymbol{e}_3$ in which $\boldsymbol{A}$ has the form (4.19). The top and bottom plates refer to planes with outward normals $\pm \boldsymbol{e}_3$, respectively, as pictured in figures 2 and 3. For these incompressible materials, the Cauchy stress is denoted $\boldsymbol{T} = -p\boldsymbol{I} + \sigma$. From the equations of motion, the pressure p for all these motions is a constant (on a connected region). The components of the extra stress in this basis are denoted σ_{ij}.

5.1.1. *Navier–Stokes fluid*

In this situation, $\sigma = 2\mu \boldsymbol{D}$, $\boldsymbol{D} = (1/2)(\nabla \boldsymbol{v} + \nabla \boldsymbol{v}^{\mathrm{T}})$, $\nabla \boldsymbol{v} = \boldsymbol{A} - \kappa t \gamma_1 \boldsymbol{e}_2 \otimes \boldsymbol{e}_3$. The viscosity is μ. This gives the non-zero stresses

$$\sigma_{12} = \mu \gamma_1, \quad \sigma_{13} = \mu \kappa, \quad \sigma_{23} = \mu(\gamma_3 - t\gamma_1 \kappa). \tag{5.2}$$

Thus, aside from the hydrostatic pressure, the top and bottom plates support only shear stress. The component of shear stress in the 2 direction on these plates changes linearly in time. There is the interesting relation $\sigma_{12}\sigma_{13} = -\mu\dot{\sigma}_{23}$. Note that σ_{23} can change sign and is unbounded. This unboundedness can be understood in terms of the unsteadiness of incompressible universal flows, or, from a more physical viewpoint, a comparison of the distance between the membranes in figures 4(*c*) and 4(*d*).

5.1.2. *Viscoelastic fluids*

We treat several typical models of viscoelastic fluids. While there is significant scepticism that any continuum model gives an accurate description of any viscoelastic fluid in a broad range of flows – in some sense justifying the molecular approach – it is interesting to observe that universal flows give unusually strong tests of the standard continuum models, also in cases in which inertia is not neglected and the flow is unsteady.

(*a*) Grade-2 fluid, with $\sigma = \alpha_1 \boldsymbol{A}_1 + \alpha_2 \boldsymbol{A}_2 + \alpha_3 \boldsymbol{A}_1^2$. Here $\boldsymbol{A}_1$ and $\boldsymbol{A}_2$ are the first two Rivlin–Ericksen tensors (Ericksen & Rivlin 1955; Pipkin & Tanner 1972). The Rivlin–Ericksen tensors $\boldsymbol{A}_i$, $i = 1, 2, \ldots$, are objective tensors defined by the formula $\boldsymbol{A}_i = \partial^i (\boldsymbol{F}_t(\tau)^{\mathrm{T}} \boldsymbol{F}_t(\tau))/\partial \tau^i|_{\tau=t}$, where $\boldsymbol{F}_t(\tau)$ is the relative deformation gradient (see the line after (4.1), and (4.2)). A grade-*n* fluid carries this expansion out to order *n* in the rate. An interesting feature of universal flows is that $\boldsymbol{A}_i = 0$ for $i \geqslant 3$. Thus, a grade-*n* fluid, $n \geqslant 2$, cannot be distinguished from a corresponding grade-2 fluid for universal motions. (This feature is also shared by some viscometric flows. This fact was noticed by Rivlin (1956), who then used it to find some exact solutions in the case of simple shearing and helical flow.) Therefore, all statements made below about universal flows of grade-2 fluids apply to fluids of any grade. The grade-2 model has been widely useful to analyse viscometric data, but, regarded as a general constitutive equation, it exhibits some unfavourable stability results when the coefficients have typical values obtained from experiment (Ting 1963; Dunn & Fosdick 1974). A reasonable view (e.g. Pipkin & Tanner 1972, p. 295) in the present case would be to regard grade-2 fluids as a good model for the stress in universal flows, because far more general models of fluids reduce to the grade-2 fluid for these flows, but not to use it to give the stress in more general flows as would necessarily arise in a stability analysis. The two non-zero Rivlin–Ericksen tensors for universal flows are

$$\left.\begin{array}{l} \boldsymbol{A}_1 = \begin{pmatrix} 0 & \gamma_1 & \kappa \\ \gamma_1 & 0 & \gamma_3 - \kappa\gamma_1 t \\ \kappa & \gamma_3 - \kappa\gamma_1 t & 0 \end{pmatrix}, \\[18pt] \boldsymbol{A}_2 = 2 \begin{pmatrix} \gamma_1^2 & 0 & \gamma_1(\gamma_3 - \kappa\gamma_1 t) \\ 0 & 0 & 0 \\ \gamma_1(\gamma_3 - \kappa\gamma_1 t) & 0 & \kappa^2 + (\gamma_3 - \kappa\gamma_1 t)^2 \end{pmatrix}, \end{array}\right\} \tag{5.3}$$

expressed in the same orthonormal basis as (4.19). The coefficients $\alpha_1, \alpha_2, \alpha_3$ can be expressed as functions of κ, γ_1, $\gamma_3 - t\gamma_1\kappa$. As in viscometric flows, universal

flows have two (typically) non-zero normal stress differences, $\sigma_{11} - \sigma_{22}$ and $\sigma_{33} - \sigma_{22}$, which vanish for the Navier–Stokes fluid. It is also worth noting that for universal flows: (*a*) σ_{22} depends on the material only through the coefficient α_3; (*b*) the normal stress differences are independent of α_1 and their dependence on α_2 and α_3 is linear. This linear system is

$$\begin{pmatrix} \sigma_{11} - \sigma_{22} \\ \sigma_{22} - \sigma_{33} \end{pmatrix} = \begin{pmatrix} 2\gamma_1^2 & \kappa^2 - (\gamma_3 - \kappa\gamma_1 t)^2 \\ -2(\kappa^2 + (\gamma_3 - \kappa\gamma_1 t)^2) & \gamma_1^2 - \kappa^2 \end{pmatrix} \begin{pmatrix} \alpha_2 \\ \alpha_3 \end{pmatrix}. \quad (5.4)$$

It is seen that this linear system can be extremely useful for partial determination of the coefficients α_2, α_3. Even better, if this linear system is solved for α_2, α_3 and the result is substituted back into the formula for the stress, and then α_1 is eliminated in favour of, say, σ_{12}, then two universal relations emerge for the extra stresses irrespective of the type of fluid in this class. In summary, universal flows reduce general viscoelastic fluids to grade-2 fluids, and give significant information about material response not contained in ordinary measurements of viscosity and normal stress differences because of the presence of three free parameters $\kappa, \gamma_1, \gamma_2$ rather than only one.

(*b*) Upper convected Maxwell (UCM), Oldroyd-B (Oldroyd 1950), Phan–Thien–Tanner (Thien & Tanner 1977) and Giesekus (Giesekus 1982) models. These models can be summarized by the constitutive equation for the extra stress,

$$\sigma = \alpha(\nabla v + (\nabla v)^{\mathrm{T}}) + (1 - \alpha)\mathbf{S}, \quad (5.5)$$

where the viscoelastic contribution to the stress satisfies the differential equation

$$w(\dot{\mathbf{S}} + (v \cdot \nabla)\mathbf{S} - (\nabla v)\mathbf{S} - \mathbf{S}(\nabla v)^{\mathrm{T}}) + \mathbf{S} + g(\mathbf{S}) = \nabla v + (\nabla v)^{\mathrm{T}}, \quad (5.6)$$

where w is the Weissenberg number and the various cases are given in table 2. Under the assumption that the flow is homogeneous, $\mathbf{S} = \mathbf{S}(t)$ only, the differential equation is easily solved for universal flows. (This assumption is widely adopted for viscometric flows as well.) For UCM and Oldroyd-B fluids, the solution of the linear equation (5.6) can be obtained analytically. For initial data beginning from the $\mathbf{S} = 0$ state, the solution is

$$\mathbf{S}(t) = \begin{pmatrix} a(t) & b(t) & c(t) \\ b(t) & d(t) & e(t) \\ c(t) & e(t) & 0 \end{pmatrix}, \quad (5.7)$$

where

$$a(t) = 2((1 - e^{-t/w})w\kappa^2 - e^{-t/w}t\kappa^2), \quad (5.8a)$$

$$b(t) = (1 - e^{-t/w})(\gamma_1 + 6w^2\gamma_1\kappa^2 + 2w\gamma_3\kappa) - e^{-t/w}(2t\gamma_3\kappa + t^2\gamma_1\kappa^2)$$
$$\quad - 2(1 + 2e^{-t/w})tw\gamma_1\kappa^2, \quad (5.8b)$$

$$c(t) = (1 - e^{-t/w})\kappa, \quad (5.8c)$$

$$d(t) = -2\left((t(\gamma_1^2 + \gamma_3^2) + t^2\gamma_1\gamma_3\kappa)e^{-t/w} + (e^{-t/w} - 1)(w\gamma_1^2 + w\gamma_3^2 \right.$$
$$\quad + 6w^2\gamma_1\gamma_3\kappa + t^2w\gamma_1^2\kappa^2 + 12w^3\gamma_1^2\kappa^2)$$
$$\quad \left. + 2(1 + 2e^{-t/w})tw\gamma_1\gamma_3\kappa + 6(1 + e^{-t/w})tw^2\gamma_1^2\kappa^2\right), \quad (5.8d)$$

$$e(t) = -(e^{-t/w} + 1)t\gamma_1\kappa + (1 - e^{-t/w}t)(2w\gamma_1\kappa + \gamma_3). \quad (5.8e)$$

Model	Value of α	Function $g(\boldsymbol{S})$
Upper convected Maxwell	0	0
Oldroyd-B	$0 < \alpha < 1$	0
Phan–Thien–Tanner	$0 < \alpha < 1$	$k(\operatorname{tr} \boldsymbol{S})\boldsymbol{S}$
Giesekus	$0 < \alpha < 1$	$k\boldsymbol{S}^2$

TABLE 2. Constitutive models of viscoelastic fluids.

Note the interesting facts about these models that $a(t)$ and $c(t)$ are independent of γ_1, γ_3 and $S_{33} = 0$ for universal flows, something that could be easily tested by a general viscometer of the type described in §4.3.1. One also sees quite unusual behaviour in these models as $t \to \infty$: while $a(t)$ and $c(t)$ asymptote to constant values, $b(t)$ and $e(t)$ have affine dependence on time and $d(t)$ is quadratic in time, implying lots of unbounded stresses in these flows.

(c) A general kind of incompressible viscoelastic fluid that includes many models is the *simple fluid* of Coleman *et al.* (1966), in which the stress is assumed to be a functional of the history of the relative deformation gradient $\boldsymbol{F}_t(z, \tau)$, $\tau \leqslant t$. Universal flows are again exact solutions. The extra stress in a simple fluid reduces to a function of $\boldsymbol{A}$ and t, because the history of the relative deformation gradient up to time t is determined by $\boldsymbol{A}$ and t. In the case where two out of three of the constants κ, γ_1, γ_3 vanish, the theory of simple fluids restricted to universal flows reduces to the theory of viscometric flows, but otherwise these motions produce new information about material response, not contained in the shear rate dependence of the viscosity and the two normal stress differences.

5.2. *Compressible heat-conducting gas*

For the compressible case, we choose a workhorse of gas dynamics, the heat-conducting viscous gas with constant specific heats. The conservation laws of mass, momentum and energy are

$$\rho_t + \operatorname{div}(\rho \boldsymbol{u}) = 0, \tag{5.9}$$

$$\rho(\boldsymbol{v}_t + \nabla \boldsymbol{v} \boldsymbol{v}) = \operatorname{div} \boldsymbol{T}, \tag{5.10}$$

$$\rho(e_t + \nabla e \cdot \boldsymbol{v}) = \boldsymbol{T} \cdot \nabla \boldsymbol{v} - \operatorname{div} \boldsymbol{q}, \tag{5.11}$$

where ρ is density, e is the internal energy, $\boldsymbol{T}$ is the Cauchy stress and $\boldsymbol{q}$ is the heat flux.

All accepted constitutive relations for heat-conducting gases have the property that, when the motion and temperature field are $\boldsymbol{v}(\boldsymbol{x}, t) = \boldsymbol{A}(\boldsymbol{I} + t\boldsymbol{A})^{-1}\boldsymbol{x}$, $\theta = \theta(t)$, then $\boldsymbol{T} = \boldsymbol{T}(t)$, $e = e(t)$, $\boldsymbol{q} = \boldsymbol{q}(t)$. (In Dayal & James (2010) we advocate that this should be a general principle satisfied by all constitutive relations.) For the motion $\boldsymbol{v}(\boldsymbol{x}, t) = \boldsymbol{A}(\boldsymbol{I} + t\boldsymbol{A})^{-1}\boldsymbol{x}$, a temperature field that only depends on t, and constitutive equations for which $\boldsymbol{T} = \boldsymbol{T}(t)$, $e = e(t)$, $\boldsymbol{q} = \boldsymbol{q}(t)$, the balance of linear momentum is an identity, and the balances of mass and energy become

$$\rho_t + \rho \operatorname{tr} \boldsymbol{A}(\boldsymbol{I} + t\boldsymbol{A})^{-1} = 0, \tag{5.12}$$

$$\rho e_t - \boldsymbol{T} \cdot \boldsymbol{A}(\boldsymbol{I} + t\boldsymbol{A})^{-1} = 0. \tag{5.13}$$

The first of these determines the density, $\rho(t) = \rho_0 \exp(-\int_0^t \operatorname{tr} \boldsymbol{A}(\boldsymbol{I} + s\boldsymbol{A})^{-1} \, \mathrm{d}s)$, and, under mild conditions on the constitutive equation for the internal energy, the latter

determines the temperature. Common constitutive equations for e and $\boldsymbol{T}$, incorporating the Stokes relation, are

$$e = c_v \theta, \tag{5.14}$$

$$\boldsymbol{T} = -p\boldsymbol{I} + \mu \left(\boldsymbol{\nabla v} + \boldsymbol{\nabla v}^{\mathrm{T}} - \tfrac{2}{3}(\mathrm{div}\,\boldsymbol{v})\boldsymbol{I} \right), \quad p = \rho R \theta, \tag{5.15}$$

with c_v being the specific heat at constant volume and R the specific gas constant. For air from room temperature to around 800 K, an accepted model is $c_v = (5/2)R$, $R = 287.06$ J kg^{-1} K^{-1}, $\mu = \mu(\theta) = 1.458 \times 10^{-6} \theta^{3/2}/(\theta + 110.3)$ Pa s. Substitution of (5.14) and (5.15) into (5.12) and (5.13) gives an ordinary differential equation for $\theta(t)$ depending parametrically on $\boldsymbol{A}$:

$$\frac{\mathrm{d}\theta}{\mathrm{d}t} = \frac{R}{c_v} \operatorname{tr} \boldsymbol{A} (\boldsymbol{I} + t\boldsymbol{A})^{-1} \theta(t) + \frac{\mu(\theta(t))}{\rho_0 c_v} \left(|\boldsymbol{A} (\boldsymbol{I} + t\boldsymbol{A})^{-1}|^2 + \operatorname{tr}((\boldsymbol{A} (\boldsymbol{I} + t\boldsymbol{A})^{-1})^2) \right.$$

$$\left. - \frac{2}{3} (\operatorname{tr}(\boldsymbol{A} (\boldsymbol{I} + t\boldsymbol{A})^{-1}))^2 \right) e^{\int_0^t \operatorname{tr} \boldsymbol{A} (\boldsymbol{I} + s\boldsymbol{A})^{-1} \, \mathrm{d}s}, \tag{5.16}$$

$$\theta(0) = \theta_0. \tag{5.17}$$

5.3. *Maxwell–Boltzmann equation*

The Maxwell–Boltzmann equation is the following equation for the molecular density function $f(t, \boldsymbol{x}, \boldsymbol{v})$:

$$\frac{\partial f}{\partial t} + \boldsymbol{v} \cdot \frac{\partial f}{\partial \boldsymbol{x}} = \int_{\mathbb{R}^3} \int_{\mathscr{S}} (f'_\star f' - f_\star f) \, \mathrm{d}S \, \mathrm{d}\boldsymbol{v}_\star. \tag{5.18}$$

The notation is

$$f'_\star = f(t, \boldsymbol{y}, \boldsymbol{v}'_\star) = f(t, \boldsymbol{y}, \boldsymbol{v}_\star - ((\boldsymbol{v}_\star - \boldsymbol{v}) \cdot \boldsymbol{e})\boldsymbol{e}), \tag{5.19a}$$

$$f' = f(t, \boldsymbol{y}, \boldsymbol{v}') = f(t, \boldsymbol{y}, \boldsymbol{v} + ((\boldsymbol{v}_\star - \boldsymbol{v}) \cdot \boldsymbol{e})\boldsymbol{e}), \tag{5.19b}$$

$$f_\star = f(t, \boldsymbol{y}, \boldsymbol{v}_\star), \tag{5.19c}$$

$$f = f(t, \boldsymbol{y}, \boldsymbol{v}), \tag{5.19d}$$

where $|\boldsymbol{e}| = 1$ depends on two angles $0 < \theta \leqslant \pi/2$, $0 \leqslant \zeta < 2\pi$ and on $\boldsymbol{v}_\star - \boldsymbol{v}$:

$$\boldsymbol{e} = \boldsymbol{e} \left(\theta, \zeta, \frac{\boldsymbol{v}_\star - \boldsymbol{v}}{|\boldsymbol{v}_\star - \boldsymbol{v}|} \right), \quad |\boldsymbol{e}| = 1. \tag{5.20}$$

The integration $\mathrm{d}S = \mathrm{d}S(\theta, \zeta; |\boldsymbol{v}_\star - \boldsymbol{v}|)$ on the right-hand side of (5.18) is, more explicitly,

$$\int_{\mathscr{S}} \cdots \mathrm{d}S = \int_0^{2\pi} \int_0^{\pi/2} \cdots \sin\theta \, \mathbb{S}(\theta, |\boldsymbol{v}_\star - \boldsymbol{v}|) \, \mathrm{d}\theta \, \mathrm{d}\zeta, \tag{5.21}$$

where $\mathbb{S}$ is the *scattering factor*.

As noted in §3, OMD solutions imply not only a macroscopic velocity field but also particular statistics of the velocity distribution. Translated into a condition on the molecular density function, this statistical relation is

$$f(t, \boldsymbol{x}, \boldsymbol{v}) = g(t, \boldsymbol{v} - \boldsymbol{A} (\boldsymbol{I} + t\boldsymbol{A})^{-1} \boldsymbol{x}). \tag{5.22}$$

Direct substitution of this ansatz into the Maxwell–Boltzmann equation (5.18) yields the following equation for $g(t, \boldsymbol{w})$:

$$\frac{\partial g}{\partial t} - \frac{\partial g}{\partial \boldsymbol{w}} \cdot \boldsymbol{A} (\boldsymbol{I} + t\boldsymbol{A})^{-1} \boldsymbol{w} = \int_{\mathbb{R}^3} \int_{\mathscr{S}} (g'_\star g' - g_\star g) \, \mathrm{d}S \, \mathrm{d}\boldsymbol{w}_\star. \quad (5.23)$$

It would be extremely interesting to study this substantially simplified equation for g.

We record the macroscopic fields that follow from the ansatz (5.22) according to the basic definitions of the kinetic theory.

(*a*) Density

$$\rho(t, \boldsymbol{x}) = m\, n(t, \boldsymbol{x}) = m \int_{\mathbb{R}^3} f(t, \boldsymbol{x}, \boldsymbol{v}) \, \mathrm{d}\boldsymbol{v} = m \int_{\mathbb{R}^3} g(t, \boldsymbol{w}) \, \mathrm{d}\boldsymbol{w} = \rho(t), \quad (5.24)$$

where, m is the molecular mass.

(*b*) Velocity

$$\begin{aligned}
\boldsymbol{v}(t, \boldsymbol{x}) = \frac{1}{n} \int_{\mathbb{R}^3} \boldsymbol{v} f(t, \boldsymbol{x}, \boldsymbol{v}) \, \mathrm{d}\boldsymbol{v} &= \frac{1}{n} \int_{\mathbb{R}^3} \boldsymbol{v} g(t, \boldsymbol{v} - \boldsymbol{A} (\boldsymbol{I} + t\boldsymbol{A})^{-1} \boldsymbol{x}) \, \mathrm{d}\boldsymbol{v} \\
&= \frac{1}{n} \int_{\mathbb{R}^3} (\boldsymbol{w} + \boldsymbol{A} (\boldsymbol{I} + t\boldsymbol{A})^{-1} \boldsymbol{x}) g(t, \boldsymbol{w}) \, \mathrm{d}\boldsymbol{w} \\
&= \boldsymbol{v}_0(t) + \boldsymbol{A} (\boldsymbol{I} + t\boldsymbol{A})^{-1} \boldsymbol{x}, \quad (5.25)
\end{aligned}$$

where $\boldsymbol{v}_0(t) = (1/n) \int_{\mathbb{R}^3} \boldsymbol{w} g(t, \boldsymbol{w}) \, \mathrm{d}\boldsymbol{w}$.

(*c*) Internal energy

$$\begin{aligned}
e(t, \boldsymbol{x}) &= \frac{1}{n} \int_{\mathbb{R}^3} \frac{1}{2} |\boldsymbol{v} - \boldsymbol{v}(t, \boldsymbol{x})|^2 f(t, \boldsymbol{x}, \boldsymbol{v}) \, \mathrm{d}\boldsymbol{v} \\
&= \frac{1}{n} \int_{\mathbb{R}^3} \frac{1}{2} |\boldsymbol{v} - \boldsymbol{v}(t, \boldsymbol{x})|^2 g(t, \boldsymbol{v} - \boldsymbol{A} (\boldsymbol{I} + t\boldsymbol{A})^{-1} \boldsymbol{x}) \, \mathrm{d}\boldsymbol{v} \\
&= \frac{1}{n} \int_{\mathbb{R}^3} \frac{1}{2} |\boldsymbol{w} - \boldsymbol{v}_0(t)|^2 g(t, \boldsymbol{w}) \, \mathrm{d}\boldsymbol{w} \\
&= \frac{1}{n} \int_{\mathbb{R}^3} \frac{1}{2} |\boldsymbol{w}|^2 g(t, \boldsymbol{w}) \, \mathrm{d}\boldsymbol{w} - \frac{1}{2} |\boldsymbol{v}_0|^2 = e(t). \quad (5.26)
\end{aligned}$$

(*d*) Cauchy stress

$$\begin{aligned}
\boldsymbol{T}(t, \boldsymbol{x}) &= -m \int_{\mathbb{R}^3} (\boldsymbol{v} - \boldsymbol{v}(t, \boldsymbol{x})) \otimes (\boldsymbol{v} - \boldsymbol{v}(t, \boldsymbol{x})) f(t, \boldsymbol{x}, \boldsymbol{v}) \, \mathrm{d}\boldsymbol{v} \\
&= -m \int_{\mathbb{R}^3} (\boldsymbol{w} - \boldsymbol{v}_0(t)) \otimes (\boldsymbol{w} - \boldsymbol{v}_0(t)) g(t, \boldsymbol{w}) \, \mathrm{d}\boldsymbol{w} \\
&= -m \int_{\mathbb{R}^3} (\boldsymbol{w} \otimes \boldsymbol{w}) g(t, \boldsymbol{w}) \, \mathrm{d}\boldsymbol{w} + \rho(t) \boldsymbol{v}_0(t) \otimes \boldsymbol{v}_0(t) = \boldsymbol{T}(t). \quad (5.27)
\end{aligned}$$

(*e*) Pressure

$$p(t, \boldsymbol{x}) = -\tfrac{1}{3} \operatorname{tr} \boldsymbol{T}(t, \boldsymbol{x}) = \tfrac{2}{3} \rho e(t), \quad (5.28)$$

which follow from the definitions for stress and internal energy above. Since temperature is proportional to internal energy in the kinetic theory, the latter is the ideal gas law.

(f) Heat flux

$$\boldsymbol{q}(t, \boldsymbol{x}) = m \int_{\mathbb{R}^3} \frac{1}{2} |\boldsymbol{v} - \boldsymbol{v}(t, \boldsymbol{x})|^2 (\boldsymbol{v} - \boldsymbol{v}(t, \boldsymbol{x})) f(t, \boldsymbol{x}, \boldsymbol{v}) \, \mathrm{d}\boldsymbol{v}$$

$$= m \int_{\mathbb{R}^3} \frac{1}{2} |\boldsymbol{w} - \boldsymbol{v}_0(t)|^2 (\boldsymbol{w} - \boldsymbol{v}_0(t)) g(t, \boldsymbol{w}) \, \mathrm{d}\boldsymbol{w}$$

$$= m \int_{\mathbb{R}^3} \frac{1}{2} |\boldsymbol{w}|^2 \boldsymbol{w} g(t, \boldsymbol{w}) \, \mathrm{d}\boldsymbol{w} + \boldsymbol{T} \boldsymbol{v}_0 - \rho e \boldsymbol{v}_0 - \frac{1}{2} \rho |\boldsymbol{v}_0|^2 \boldsymbol{v}_0 = \boldsymbol{q}(t). \quad (5.29)$$

Formally, the balance laws of continuum mechanics are satisfied by these quantities, i.e.

$$\rho_t + \mathrm{div}(\rho \boldsymbol{v}) = 0, \quad (5.30)$$

$$\rho(\boldsymbol{v}_t + \nabla \boldsymbol{v} \boldsymbol{v}) = \mathrm{div} \, \boldsymbol{T}, \quad (5.31)$$

$$\rho(e_t + \nabla e \cdot \boldsymbol{v}) = \boldsymbol{T} \cdot \nabla \boldsymbol{v} - \mathrm{div} \, \boldsymbol{q}. \quad (5.32)$$

For the invariant solutions, these become, using the evaluations above,

$$\rho_t + \rho \, \mathrm{tr} \, \boldsymbol{A} \, (\boldsymbol{I} + t\boldsymbol{A})^{-1} = 0, \quad (5.33)$$

$$\rho(\boldsymbol{v}_{0\,t} + \boldsymbol{A} \, (\boldsymbol{I} + t\boldsymbol{A})^{-1} \boldsymbol{v}_0) = 0, \quad (5.34)$$

$$\rho e_t - \boldsymbol{T} \cdot \boldsymbol{A} \, (\boldsymbol{I} + t\boldsymbol{A})^{-1} = 0. \quad (5.35)$$

The quantities $\rho, \boldsymbol{v}_0, e, \boldsymbol{T}$ in (5.33)–(5.35) are functions of t only. Equations (5.33)–(5.35) have the same structure as (5.12) and (5.13), except for the balance of linear momentum. However, by direct calculation we note that the solution of the balance of linear momentum in (5.33)–(5.35), subject to $\boldsymbol{v}_0(0) = \boldsymbol{c}$, is

$$\boldsymbol{v}_0(t) = \boldsymbol{c} - t\boldsymbol{A} \, (\boldsymbol{I} + t\boldsymbol{A})^{-1} \boldsymbol{c}. \quad (5.36)$$

To simplify things we can take $\boldsymbol{c} = 0$. At the level of the molecular density function g, this is equivalent to noticing that if $g(t, \boldsymbol{w})$ satisfies (5.23) then so does $g(t, \boldsymbol{w} + t\boldsymbol{A} \, (\boldsymbol{I} + t\boldsymbol{A})^{-1} \boldsymbol{c} - \boldsymbol{c})$. Thus, without loss of generality we can assume that the first moment of the initial datum for g vanishes: $\int \boldsymbol{w} g(0, \boldsymbol{w}) \, d\boldsymbol{w} = \boldsymbol{c} = 0$. Then, by (5.36), it will vanish for all time. With $\boldsymbol{v}_0(t) = 0$ the quantities $\rho, e, \boldsymbol{T}, \boldsymbol{q}$ are interpretable as various moments of g, and (5.33)–(5.35) become (5.12) and (5.13).

While (5.33)–(5.35) are now formally identical to those of a compressible heat-conducting gas, there is the significant difference that there are no exact constitutive equations in the kinetic theory. However, in view of the ideal gas law (5.28), equation (5.35) gives an interesting universal relation between various stresses for universal solutions. More generally, the reduced equation (5.23) may well be amenable to analytical or simple numerical solution. The argument could well be made, however, based on the ability to use more accurate models of atomic force than possible with the kinetic theory, that a direct attack at the molecular level using OMD would be better.

There is a simple H-theorem for universal flows. Defining the H function (often interpreted as the negative of the entropy) by $H(t, \boldsymbol{x}) = \int f \log f \, \mathrm{d}\boldsymbol{v} = \int g \log g \, \mathrm{d}\boldsymbol{w}$, it follows by a variant of the usual argument (i.e. multiply the Maxwell–Boltzmann equation by $\log f$, integrate over $\boldsymbol{v} \in \mathbb{R}^3$ and use monotonicity of the log function) that the following simple form of the H-theorem emerges:

$$\frac{\partial H}{\partial t} + \mathrm{tr}(\boldsymbol{A} \, (\boldsymbol{I} + t\boldsymbol{A})^{-1} H \leqslant 0. \quad (5.37)$$

For incompressible flows the trace term vanishes and we get the simple statement that the H function (defined in this way) increases. Typically, there is strict inequality in (5.37). It is interesting to note that, despite the fact that the kinetic theory is not time-reversible, as follows from strict inequality in (5.37), while molecular dynamics (2.6) and (2.7) is time-reversible, the kinetic theory inherits exactly the invariant manifold of molecular dynamics that is the basis of OMD.

This invariant manifold is also faithfully inherited by the Langevin equation for beaded chains in a shear flow, by the large eddy simulation equations of turbulence (Dayal & James 2010) and by the Liouville equation of non-equilibrium statistical mechanics (author's unpublished observations).

6. Summary

The purpose of this paper is to suggest a certain nine-parameter family of flows as an alternative basis for the determination of fundamental properties of complex fluids. The main reason behind this suggestion is that, at atomic level, there is a corresponding molecular simulation method having a form that can be prescribed independent of the details of atomic forces, and, at continuum level, the associated macroscopic flows $v(x, t) = A(I + tA)^{-1}x$ are exact solutions of the equations of motion for every accepted model of fluid. Since this goal is primarily experimental in nature but the arguments are largely theoretical, we collect in this summary practical recommendations that may be of use to the experimental rheology community.

In §4.2 we solved the problem of whether, for any choice of the assignable 3×3 matrix A, such a flow could be confined by (possibly curved) surfaces moving as rigid bodies, this being a simplifying design feature. In all cases that such rigid surfaces confine these flows, A is necessarily a matrix of rank one, i.e. $A = a \otimes n$. (In rectangular Cartesian components, $A_{ij} = a_i n_j$. Without loss of generality take $|n| = 1$.) The generic case of such a flow is illustrated in figure 1. Besides the special case of plane Couette flow ($a \cdot n = 0$), all such cases correspond to compressible flows. Evidently, the associated devices are best suited to a variety of interesting questions that arise in aerodynamics and combustion. Referring to figure 1, the main practical consideration is to move the leading edge of plate 1 *at constant velocity* towards (or away from) the stationary plate 2. For slow motions there is an issue of preventing the fluid escaping at the top and bottom. This could be handled by confining plates as shown, or, more accurately, by deformable membranes attached to the edges of plates 1 and 2 and backed up by lubricated stiff plates. For relatively slow flows in which wave propagation effects are not important, a natural suggestion is to use a feedback control system, such as those built in to standard servohydraulic testing systems, to control the motion of plate 1.

The main important parameters for the device pictured in figure 1 are the speed $|a|$ of plate 1 and the angle $\arccos(a \cdot n/|a|)$. As an example of an explicit continuum-level solution corresponding to these flows, the solution of the equations of mass, momentum and energy for a simple heat-conducting ideal gas with constant specific heats and a typical explicit temperature-dependent viscosity is given in §5.2. More interesting cases are pressure-induced dissociation or combustion of a suitable gas mixture. It is still expected that the temperature is only a function of time in those cases, as well as quantities such as the extent of reaction. This pure time dependence, independent of position, is particularly attractive for diagnostics. Such cases are within the scope of molecular dynamics simulations using OMD with reasonably sophisticated atomic forces.

We have discussed briefly the high-speed case in which plate 1 approaches Mach 1 or higher. This interesting case needs further study because of the management of transients and the impossibility of using a standard control system. There is a potentially useful literature (e.g. Kim, Clifton & Kumar 1977) on the pressure-shear impact experiment in solids where these two problems have been overcome by clever design.

The general incompressible case is analysed in §4.3. Except for the choice of orthonormal basis (which only matters for anisotropic fluids such as liquid crystals), there are three free parameters in this case, $\kappa, \gamma_1, \gamma_3$. If $\kappa\gamma_1 \neq 0$ such flows exhibit vortex stretching. These flows do not rigidly deform any surfaces. However, the general case of such flows can be pictured as in figure 4, where the shear rates γ_1, γ_3, τ are illustrated. Panels (*a*) and (*b*) of figure 4 give a top view, while (*c*) and (*d*) are end views. In our view the key design aspects are: obtaining high-quality, uniform, highly stretchable membranes; backing the membranes up by stiff plates or possibly density-matched fluids to prevent unwanted out-of-plane motions of these membranes; and arranging that the gap w between membranes at $t = 0$ is sufficiently small so that substantial shearing occurs. As a technically simpler special case that still retains vortex stretching, one could put $\gamma_3 = 0$. To simplify diagnostics, note that a suitable Galilean transformation keeps the midpoint of the membranes in figure 4(*c,d*) stationary. Explicit forms of stresses in these flows from some standard models of incompressible complex fluids are given in §5.1. A rheometer of the type sketched in figure 4 would give major new critical tests that could sort out the applicability of these models.

Acknowledgements

REFERENCES

BENTLEY, B. J. & LEAL, L. G. 1986 A computer-controlled four-roll mill for investigations of particle and drop dynamics in two-dimensional linear shear flows. *J. Fluid Mech.* **167** (1), 219–240.

CHAKRABORTY, P., BALACHANDAR, S. & ADRIAN, R. J. 2005 On the relationships between local vortex identification schemes. *J. Fluid Mech.* **535** (1), 189–214.

CHAN, N. Y., CHEN, M. & DUNSTAN, D. E. 2009 Elasticity of polymer solutions in Couette flow measured by fluorescence resonance energy transfer (FRET). *Eur. Phys. J. E: Soft Matter Biol. Phys.* **30** (1), 37–41.

CHONG, M. S., PERRY, A. E. & CANTWELL, B. J. 1990 A general classification of three-dimensional flow fields. *Phys. Fluids* **2** (5), 765–777.

COLEMAN, B. D., MARKOVITZ, H. & NOLL, W. 1966 *Viscometric Flows of Non-Newtonian Fluids: Theory and Experiment*. Springer.

CROWLEY, D. G., FRANK, F. C., MACKLEY, M. R. & STEPHENSON, R. G. 1976 Localized flow birefringence of polyethylene oxide solutions in a four roll mill. *J. Polym. Sci.* **14** (6), 1111–1119.

DAYAL, K. & JAMES, R. D. 2010 Nonequilibrium molecular dynamics for bulk materials and nanostructures. *J. Mech. Phys. Solids* **58** (2), 145–163.

DUMITRICA, T. & JAMES, R. D. 2007 Objective molecular dynamics. *J. Mech. Phys. Solids* **55** (10), 2206–2236.

DUNN, J. E. & FOSDICK, R. L. 1974 Thermodynamics, stability, and boundedness of fluids of complexity 2 and fluids of second grade. *Arch. Ration. Mech. Anal.* **56** (3), 191–252.

ERICKSEN, J. L. & RIVLIN, R. S. 1955 Stress–deformation relations for isotropic materials. *Arch. Ration. Mech. Anal.* **4**, 323–425.

EVANS, D. J. & MORRISS, G. P. 2008 *Statistical Mechanics of Nonequilibrium Liquids*. Cambridge University Press.

GIESEKUS, H. 1962 Stromungen mit konstantem Geschwindigkeitsgradienten und die Bewegung von darin suspendierten Teilchen. *Rheol. Acta* **2** (2), 101–112 and 112–122.

GIESEKUS, H. 1982 A unified approach to a variety of constitutive models for polymer fluids based on the concept of configuration-dependent molecular mobility. *Rheol. Acta* **21** (4), 366–375.

HALLER, G. 2005 An objective definition of a vortex. *J. Fluid Mech.* **525**, 1–26.

HUNT, J. C. R., WRAY, A. A. & MOIN, P. 1988 Eddies, stream, and convergence zones in turbulent flows. *Report CTR-S88*. Center for Turbulence Research.

JEONG, J. & HUSSAIN, F. 1995 On the identification of a vortex. *J. Fluid Mech.* **285** (1), 69–94.

KIM, K. S., CLIFTON, R. J. & KUMAR, P. 1977 A combined normal- and transverse-displacement interferometer with an application to impact of y-cut quartz. *J. Appl. Phys.* **48** (10), 4132–4139.

KRAYNIK, A. M. & REINELT, D. A. 1992 Extensional motions of spatially periodic lattices. *Intl J. Multiphase Flow* **18** (6), 1045–1059.

LAGNADO, R. R. & LEAL, L. G. 1990 Visualization of three-dimensional flow in a four-roll mill. *Exp. Fluids* **9** (1), 25–32.

LEES, A. W. & EDWARDS, S. F. 1972 The computer study of transport processes under extreme conditions. *J. Phys. C: Solid State Phys.* **5**, 1921.

OLDROYD, J. G. 1950 On the formulation of rheological equations of state. *Proc. R. Soc. Lond. Ser.* A. *Math. Phys. Sci.* **200** (1063), 523.

PARLATO, P. 1969 Non-viscometric flows of viscoelastic liquids. Master's thesis, Department of Chemical Engineering, University of Delaware.

PIPKIN, A. C. & TANNER, R. I. 1972 A survey of theory and experiment in viscometric flows of viscoelastic liquids. *Mech. Today* **1**, 262–321.

RIVLIN, R. S. 1956 Solution of some problems in the exact theory of visco-elasticity. *J. Ration. Mech. Anal.* **5**, 179.

TAYLOR, G. I. 1934 The formation of emulsions in definable fields of flow. *Proc. R. Soc. Lond. Ser.* A **146** (858), 501.

THIEN, N. P. & TANNER, R. I. 1977 A new constitutive equation derived from network theory. *J. Non-Newtonian Fluid Mech.* **2** (4), 353–365.

TING, T. W. 1963 Certain non-steady flows of second-order fluids. *Arch. Ration. Mech. Anal.* **14** (1), 1–26.

TODD, B. D. & DAIVIS, P. 2007 Homogeneous non-equilibrium molecular dynamics simulations of viscous flow: techniques and applications. *Mol. Simul.* **33** (3), 189–229.

TORZA, S. 1975 Shear-induced crystallization of polymers. I. The four-roller apparatus. *J. Polym. Sci.* **13** (1), 43–57.

YIN, W. L. & PIPKIN, A. C. 1970 Kinematics of viscometric flow. *Arch. Ration. Mech. Anal.* **37** (2), 111–135.